January 10, 2000

MEMORANDUM TO: Susan F. Shankman, Deputy Director
Licensing and Inspection Directorate
Spent Fuel Project Office, NMSS

FROM: Mary Jane Ross-Lee, Project Manager ORIGINAL SIGNED BY /s/
Licensing Section
Spent Fuel Project Office, NMSS

SUBJECT: SUMMARY OF DECEMBER 16, 1999, MEETING WITH BNFL FUEL SOLUTIONS AND CONSUMERS ENERGY

On December 16, 1999, the Spent Fuel Project Office (SFPO) staff met with representatives from BNFL Fuel Solutions (BFS) and Consumers Energy regarding the issues remaining in the review of the Wesflex Spent Fuel Management System (Wesflex System). This meeting specifically addressed questions relating to high burnup fuel cladding integrity, creep methodology, thermal (including peak rod pressure calculations), confinement, shielding and structural. Consumers Energy plans to use the Wesflex System at its Palisades and Big Rock Point plants. An attendance list is included as Attachment 1. The meeting was noticed on December 7, 1999.

Background

The Wesflex System is a spent fuel storage cask system. Westinghouse Electric submitted the Wesflex System storage application for approval on February 3, 1998, as supplemented. Subsequently, the Wesflex System was purchased by BFS. The staff completed its second round review of the storage application and issued an RAI on August 24, 1999. BFS's response to the RAI was received November 1, 1999. The staff is to issue a preliminary Safety Evaluation Report (SER) and Certificate of Compliance (CoC) in March 2000.

Meeting Discussion

The topics discussed at the meeting are included in the agenda (Attachment 2). Additional staff comments on the cladding temperature limit, high burnup fuel analysis, and structural are included (Attachment 3). BFS is to provide a letter and schedule of commitment for responses by December 20, 1999.

During the course of the meeting, no regulatory decisions were requested or made.
Docket No. 72-1026
Attachments: 1. Attendance List
2. Agenda
3. Staff Comment Handouts

DISTRIBUTION:

Dockets	NRC File Center	PUBLIC	NMSS r/f	SFPO r/f
RLandsman, RIII	BJorgensen, RIII	PHarris, NRR	BSchaaf, NRR	SGagner, OPA

SFPO ELECTRONIC DISTRIBUTION:
NRC Attendees WHodges EWBrach

OFC:	SFPO	E	SFPO	E	SFPO						
NAME:	MJRoss-Lee		VLThaipe		CRChappell						
DATE:	01/6/00		01/10/00		01/10/00						

G:\WESFLEX\MEETINGS\121699MTGSUM.wpd **OFFICIAL RECORD COPY**

DFO3

PDR ADOCK 07201026

Meeting between Nuclear Regulatory Commission
and BNFL Fuel Solutions

December 16, 1999

ATTENDEES

Name	Organization
Mary Jane Ross-Lee	NRC/NMSS/SFPO
Andrew Barto	NRC/NMSS/SFPO
Chris Brown	NRC/NMSS/SFPO
Herb Conrad	NRC/NMSS/SFPO
Adelaide Giantelli	NRC/NMSS/SFPO
Kim Gruss	NRC/NMSS/SFPO
Jack Guttmann	NRC/NMSS/SFPO
Henry Lee	NRC/NMSS/SFPO
Bernie White	NRC/NMSS/SFPO
Carl Beyer	PNNL
ER Gilbert	PNNL
Tom Michener	PNNL
Greg Bankin	BNFL/Q-Metrics
John Bowen	BNFL Fuel Solutions
Jim Hopf	BNFL Fuel Solutions
Bob Quinn	BNFL Fuel Solutions
Garry Thomas	Polestar Applied Tehcnology
Albert Machiels	EPRI
Phil Flenner	Consumers Energy
Dave Morse	Consumers Energy
Dave Waters	Consumers Energy
John Foster	Westinghouse CNFD
Senri Tabahashi	IHI
Steve Schulin	The Ibex Group

Attachment 1

Spent Fuel Project Office Meeting with
BNFL Fuel Solutions

December 16, 1999, 8:00 am - 3:00 pm

AGENDA

- Wesflex Storage System
  - High Burn Up Fuel
  - Creep Methodology
  - Thermal, including peak rod pressure calculations
  - Confinement
  - Shielding
  - Structural
  - Miscellaneous
- Summarize and discuss commitments and schedule

Attachment 2

Attachment 3

Talking Points for Clarification on Cladding Temperature Limit and High Burnup Fuel Analyses

A. General Questions

1. With reference to Table 6-1 of CMPC.1505.010, a comparison of the maximum allowable temperatures calculated with the creep correlation and the CSFM method shows a 6-9°C temperature difference for all of the PWR fuel. However, for Big Rock Point, there is almost a 30°C temperature difference between the temperatures calculated from the creep correlation approach the CSFM method. Please explain why the temperature difference for the Big Rock Point Fuel is so much larger.

2. With reference to RAI #2, BFS Response 2, it is suggested that the wastage factor be calculated based on 100 μm of corrosion and a Pilling- Bedworth (P-B) ratio of 1.7. The NRC has not approved the use of a P-B ratio other than the theoretical value of 1.56 for in-reactor analyses. Correct the analyses (i.e., cladding hoop stresses) using a P-B ratio of 1.56.

3. With reference to WCAP-15168, Figure 4-16 is based on SNF that has been discharged for 9.1 years. Is the temperature history shown in Figure 4-16 conservative for fuel that has been discharged for more than 9.1 years? Will older fuel always be at a sufficiently low temperature that the 9.1 fuel age is always bounding?

4. The rod stresses in Table 4.3-2 of SAR Section 4.3.2 (Rev. 3) seem to be 10-17% lower than those of the previous revision of the SAR (Rev. 2). Why are the rod stresses now lower?

5. To address our concerns about preferential loading, perform strain calculations for mixed loading of fuel assemblies in a cask (i.e., 5-year cooled fuel adjacent to 15-year cooled fuel) to show that the 1% strain limit is not exceeded for different ages of fuel at the limiting conditions.

B. Creep Methodology

1. As a general comment, the RAI #2 responses and the Supplement to RAI #2 refer to data or data sets but do not provide the references for these data. Provide the references for the following:

- On Page 5 of RAI #2, the sentence starting with, "Typical uniform oxide thicknesses for discharge fuel are in the 50-60 micron range even at the highest burnup and hydrogen pickup fractions are well below those of PWRs."

- On Page 8 of RAI #2, the two sentences in the last paragraph on this page.

- On Page 9 of RAI #2, the three sentences in the first paragraph on the page starting with, "In the irradiated condition, the yield and ultimate strengths also increase...". And, the first sentence of the second paragraph which starts with, "It should be noted that the few very low ductility results observed..."

- On Page 9 of RAI #2, the sentence starting with, "However, most mechanical property measurements on irradiated cladding are conducted on samples which exhibit..."

- On Page 10 of RAI #2, the sentence starting with, "The absence of radial hydrides, even in cladding with circumferential stressing, ..."

- On Page 11 of RAI #2, the sentence starting with, "As can be seen in many experimental steady-state Zircaloy creep data sets, ..."

- On Page 14 of RAI #2, the sentence starting with, "As a significant added factor, there is experimental evidence the Zircaloy obeys the strain hardening rule..."

- On Page 18 of the Supplement to RAI #2, the 3 sentences in the third paragraph starting with, "The out-reactor creep of cold worked, stress relieved (CWSR) Zircaloy-4 fuel rod tubing (cladding has been measured and modeled."

2. In reference to RAI #2, BFS Response No. 8, Bullet 1, you state that, "There is no indication in the data that the limits of secondary creep have been reached in that time frame." The concern is that under certain conditions the cladding material may experience tertiary creep in which the strain rates increase with time and lead to failure of the cladding. Unfortunately, there are few long term data showing which conditions (e.g., stress, temperature, time, etc.) lead to tertiary creep. Please strengthen your argument by consider the effects of tertiary creep (i.e., the damage resulting from tertiary creep) on cladding integrity during storage.

3. In the Supplement to RAI #2, Section 3, please explain what is meant by the last sentence of this section which starts with, "At the same time, the canister heat load to values reported in Table 3-1 will substantially decrease, ..."

4. The factor of 10 between the Spilker equation for unirradiated Zry-4 and the irradiated FRG-2 creep data does not appear to be defensible. The difference between the unirradiated FRG-2 (WCAP-15168, Figure 4-2) and the irradiated (WCAP-15168, Figure 4-4) creep data are shown to range from a factor of 1.4 to a factor of 2.5 for a stress of ~87 MPa and 395°C. Examination of other published data show the ratio of unirradiated to irradiated creep to be strongly stress dependent. The values of the creep reduction factor (of unirradiated to irradiated creep) in the Schaeffler-LePichon et al. 1997 work decrease from ~55 at 460 MPa to ~6 at 310 MPa at 350°C. Further, the value at 300°C and 310 MPa is ~9 (Fidleris 1979 ASTM STP 681).

C. Storage of High Burnup Fuel

1. With reference to WCAP-15168, Section 3.1.2 suggests that more than 90% of discharged fuel will have oxide thicknesses less than 100 μm and the majority of fuel is currently below 50 μm thickness. This seems to be misleading because current and future fuels will have higher fuel duties and higher burnups than older fuel. This will increase the oxide thicknesses such that the majority of fuel will have oxide thicknesses greater than 50 to 60 μm.

2. With reference to WCAP-15168, Section 3.2 suggests that hydrogen levels up to 600 ppm do not significantly reduce cladding ductilities at both in-reactor temperatures and at lower temperatures close to room temperatures as indicated in the preceding comment (Note C1). The uniform strains presented in Tables 3-1 and 3-2 of the WCAP report show burst and tensile strain ranges less than 1% when hydrogen levels are above 300 ppm. In order for BFS to demonstrate that the 1% strain limit is bounding for high burnup rods with oxide thicknesses up to 100 μm, long term creep data are needed that are prototypic of the BFS limiting storage conditions.

3. With reference to WCAP-15168, the burnup and corrosion level of the long term creep data of irradiated cladding, as presented in the figures of Section 4 of the WCAP report, are significantly lower than the maximum corrosion and burnup levels of higher burnup fuels. There are high burnup cladding data and unirradiated cladding data at 350°C that suggest a hydride rim typical of high burnup cladding with hydrogen levels greater than 1000 ppm in the rim significantly reduces the cladding ductility. The BFS creep methodology may be able to estimate the maximum cladding temperature limits for high burnup fuel if appropriate parameters and bounding conditions are applied. However, no creep data for fuel cladding with high concentrations of hydrides have been provided. The presence of a brittle hydride rim is expected to increase the potential for incidence and propagation of through-wall cracks.

4. Recent pellet-cladding mechanical interaction (PCMI) data from reactivity insertion tests, as well as burst and tensile tests, of cladding with corrosion thicknesses greater than 70 μm shows that failure of high hydrogen concentration cladding is initiated by cracking in the brittle hydride rim. It is likely that this will be a failure mechanism for high-burnup spent fuel cladding. In general, BFS has not considered this failure mechanism or a failure mechanism that is associated with the presence of hydride blisters on the cladding. Please propose an approach to account for crack initiation in the hydride rim, and/or at hydride blisters, and failure propagation through the remaining ductile metal. Further, evaluate the effects these failure mechanisms may have on the integrity of the cladding during storage.

5. On Page 9 of RAI #2, reference is made to a creep study with hydrided unirradiated Zircaloy 4 (i.e., a paper written by Bouffioux and Rupa). Our review of this work revealed that the results of this study cannot be extrapolated to high burnup fuels (i.e., hydrided irradiated Zircaloy 4) for the following reason. For short test periods (< 30 hours), the ductile Zr-4 matrix containing hydrides is like a composite with may reduce the creep rate and slightly increase the fracture strain. However, in high burnup fuel, there is a concentration gradient of hydrogen across the thickness of the cladding with a highly concentrated region of

hydrides (i.e., a hydride rim) that is brittle and may accommodate less strain to failure. Therefore, relevant data are needed to evaluate BFS's unverified assumption that the data from hydrided unirradiated Zircaloy 4 can be extended to include hydrided irradiated material.

6. With respect to RAI #2, BFS Response 10 to Section 4.5.3 of the WCAP report, BFS notes that NRC has accepted the Westinghouse 1% permanent strain limit for steady-state fuel operation. There are NRC staff positions on a 1% strain limit. This position generally treats the 1% as the total strain, i.e., the sum of elastic plus plastic strains. However, this strain limit would be questioned today by NRC based on the available ductility data from (1) high burnup rods with oxide thicknesses between 70 to 100 μm (with the observed hydride rim), and (2) unirradiated cladding with a simulated hydride rim currently available to NRC.

   The NRC is aware of unirradiated cladding data with a hydride rim similar to high burnup rods that demonstrate a significant reduction in cladding ductility when a hydride rim is introduced in unirradated cladding. Additionally, the uniform strain measured for high burnup fuel having 100 microns of corrosion is consistently <1%, where the brittle hydride rim associated with this amount of corrosion is a likely factor in the reducing the uniform strain. Based on this information BFS would be required to produce additional data to support that the 1% permanent strain limit is bounding for the high burnup fuel. Further, for BFS to demonstrate that the 1% strain limit is bounding for high burnup rods with oxide thicknesses up to 100 μm, additional long term creep data would be needed that are prototypic of BFS limiting storage conditions.

7. With respect to RAI #2 and the Supplement to RAI #2, BFS discusses the application of the Monkman-Grant constant to dry storage evaluation. In general, determination of the Monkman-Grant constant requires measurements of the time to breach and minimum or steady-state creep rate. These data have not been made available for irradiated Zircaloy 4. While the technical basis for the Monkman-Grant constant for unirradiated Zircaloy 2 and Zircaloy 4 (i.e., constant >0.3) has been evaluated for the fracture mechanism of cavitation growth by dislocation creep, it is unclear how the Monkman-Grant constant derived from tests of unirradiated Zircaloy 4 is applicable to irradiated Zircaloy 4. Furthermore, there are no data for high burnup fuel cladding to determine if crack initiation in a brittle hydride rim may affect the value of the Monkman-Grant constant.

Structural

WSNF-201, W21 Canisters

1. Drawing No. W21-122 should be revised to show either the outside dimensions of the Guide Tube or show the width of the Neutron Absorber Wrapper.

2. Revise second paragraph On Page 3.7-21, to be consistent with analysis performed. The paragraph stated that the W21 canisters are able to withstand an equivalent static bottom end drop acceleration of 60g without affecting the canister primary safety functions. Also, it said that the transfer cask is shown to withstand the end drop load of 90g. The W21 canisters are evaluated for 50g end drops and no end drop evaluation of the transfer cask has been provided in the WSNF-200 SAR.

WSNF-203, W74 Canisters

1. Page 3.7-10, stated that the maximum primary membrane and primary membrane plus bending stresses in the W74 support tube due to the 50g end drop are 18.8 ksi and 19.7 ksi. However, in the Buckling Evaluation at the bottom of Page 3.7-10, It stated that the maximum support tube stresses result from the 50g end drop load are determined by hand calculations and that the maximum support tube axial stress is 22.1 ksi. Those statements are not consistent. Revise the SAR.

WSNF-201 and WSNF-203

1. Provide the boundary conditions and the applied loads for the finite element model used to evaluate the bottom end region of the canisters under the storage cask bottom end drop loading condition.

Voids + Cavities

Adamson, RB, RP Tucker, and V. Fidleris. 1982. ASTM STP 754, 208-234

GILBERT, RW, K. FARRELL, and CE Coleman. 1979. J. Nucl. Mater. 84: 137-148

GRIFFITHS, M, RW GILBERT, V FIDLERIS, RP TUCKER, and RB ADAMSON, ~~1987~~ 1987, J. Nucl. Mater. 150:159-168

GRIFFITHS, M. J NUCL. MATER. 159: 190-218

GRIFFITHS, M, R STYLES, C WOO, F Phillipp, and W Frank, 1994, J. Nucl. Mater. 208: 324-334

HOLT, RA, RW GILBERT, and V FIDLERIS, 1982, ASTM-STP-782, 234-250

Keusseyan, R, C Hu, an C Li. 1979. J. Nucl. Mater. 80: 390-392

Comparison of Spilker Time Exponent with FRG-2 Unirradiated and Irradiated Creep Strain Data

The following figure compares the strain-time curves for the two bounding unirradiated FRG-2 test series from Figure 4-2 on Page 4-17 with the strain-time curves for the two bounding irradiated FRG-2 test series from Figure 4-4 on Page 4-19. The data are presented on log-log plots which is the format used by Spilker to evaluate the value of the time exponent from the slope.

The results show consistency in the values of the exponents on time for the unirradiated FRG-2 tests with the Spilker-equation approach in that the values of the time exponents are <1 (m = <1). However, for the irradiated FRG-2 data, the time dependence does not follow the Spilker equation. The values of the time exponents are >1 (m = >1). Consequently it appears that extrapolation of these data on the Spilker type correlation plot results in the creep strain curves for irradiated Zry-4 crossing over and above the creep strains for unirradiated Zry-4 in less than 20,000 hours under isothermal conditions. Extrapolation of the irradiated FRG-2 data on this plot suggests that the 1% strain limit might be reached in less than 20,000 hours under isothermal conditions.

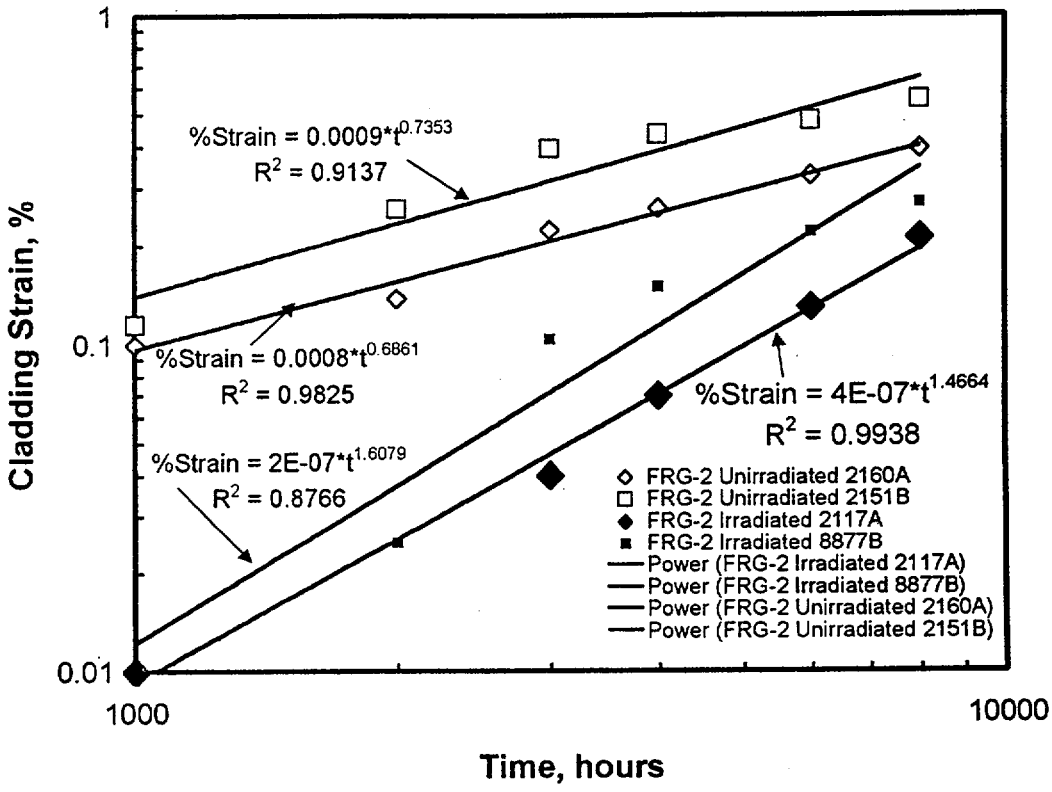

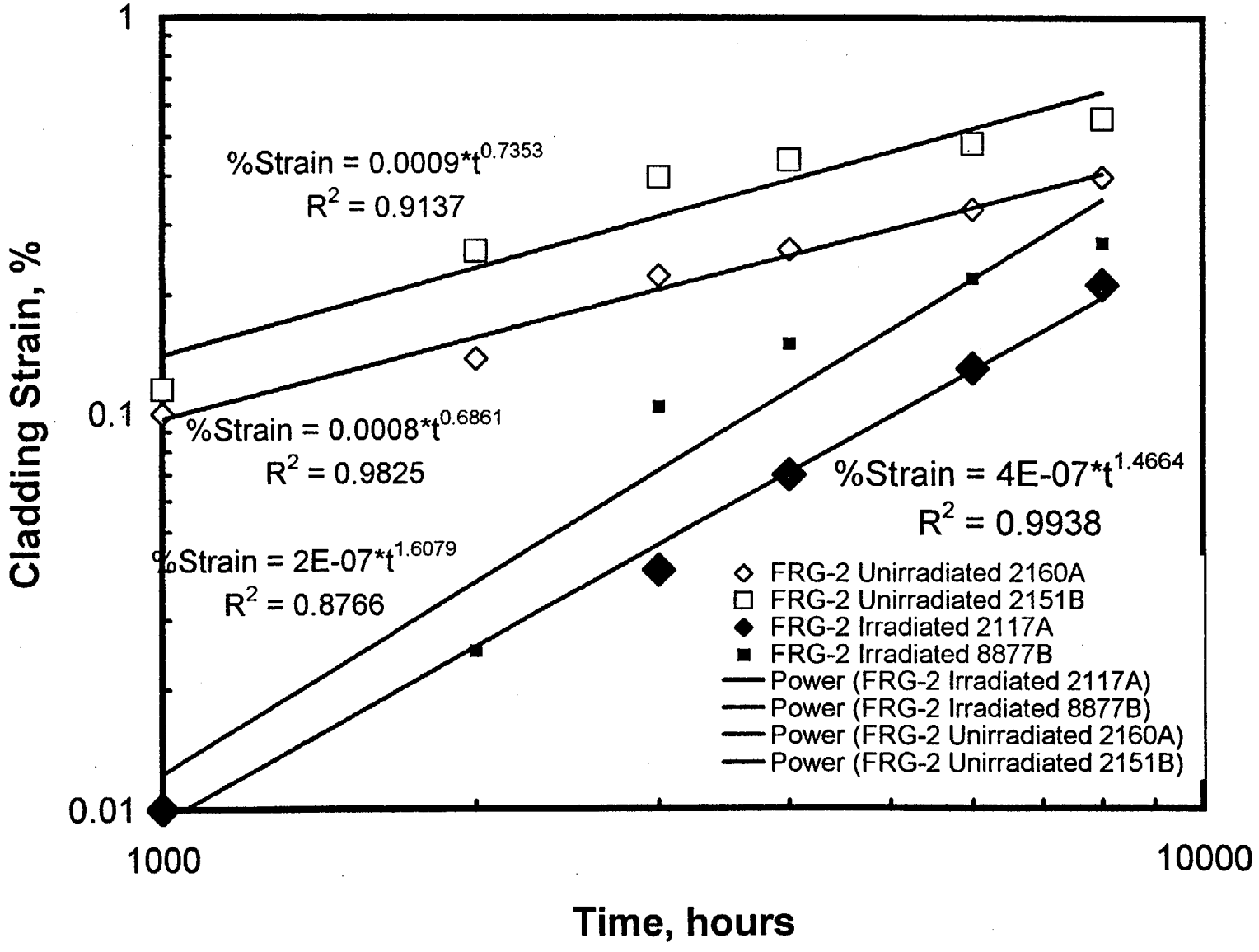
1
0.1
0.01
1000
10000
Cladding Strain, %
Time, hours
%Strain = 0.0009*t^0.7353
R2 = 0.9137
%Strain = 0.0008*t^0.6861
R2 = 0.9825
%Strain = 2E-07*t^1.6079
R2 = 0.8766
%Strain = 4E-07*t^1.4664
R2 = 0.9938
FRG-2 Unirradiated 2160A
FRG-2 Unirradiated 2151B
FRG-2 Irradiated 2117A
FRG-2 Irradiated 8877B
Power (FRG-2 Irradiated 2117A)
Power (FRG-2 Irradiated 8877B)
Power (FRG-2 Unirradiated 2160A)
Power (FRG-2 Unirradiated 2151B)

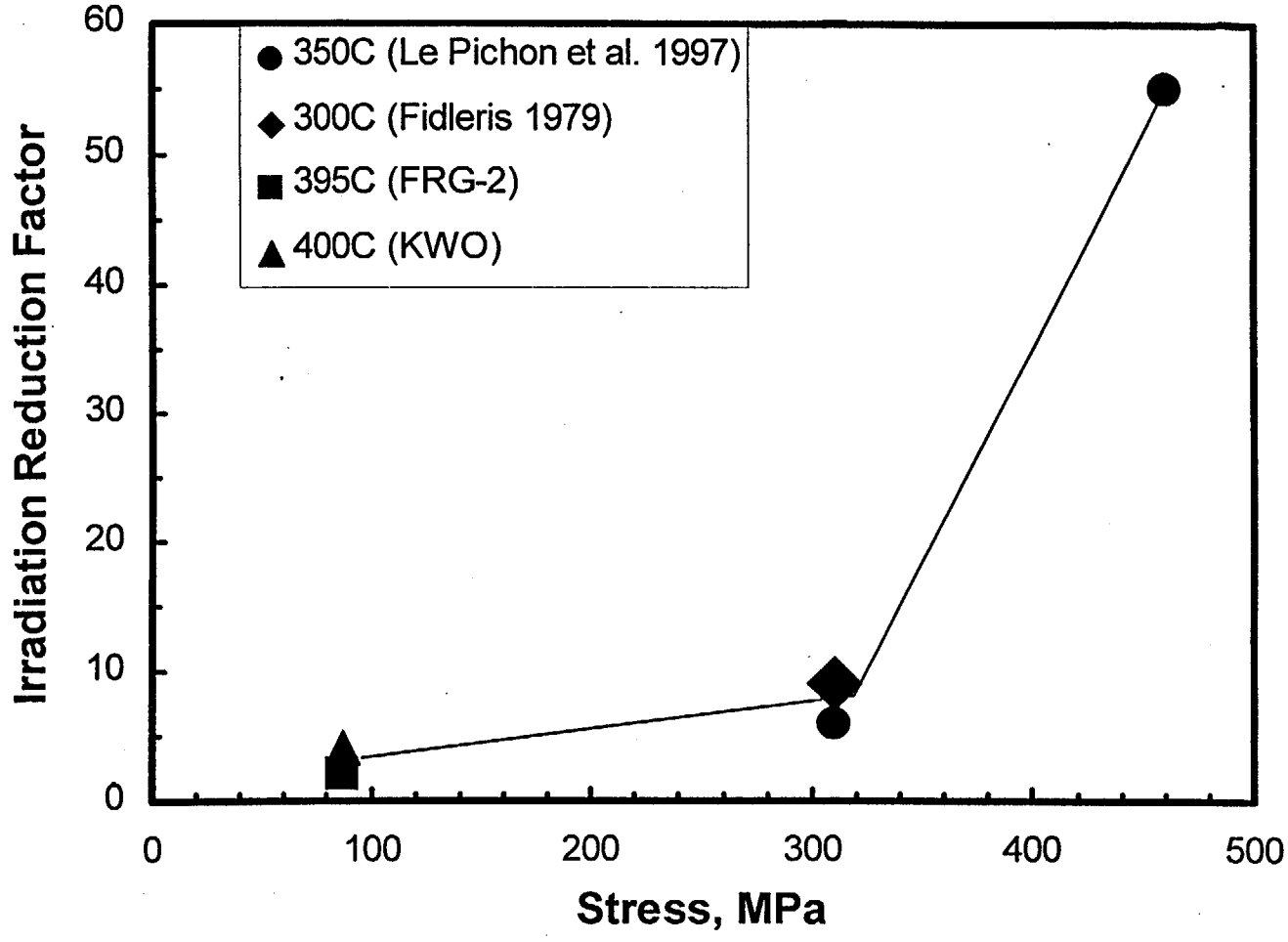

Effect of Stress on Creep Reduction Factor for Unirradiated vs. Irradiated Zry-2

Battelle

U.S. Department of Energy
Pacific Northwest National Laboratory

Hydride Characteristics

MATERIALS

LOW-TEMPERATURE RUPTURE BEHAVIOR OF ZIRCALOY-CLAD PRESSURIZED WATER REACTOR SPENT FUEL RODS UNDER DRY STORAGE CONDITIONS

ROBERT E. EINZIGER *Westinghouse Hanford Company, P.O. Box 1970 Mail Stop W/A-40, Richland, Washington 99352*

RAJIV KOHLI *Battelle Columbus Laboratories, 505 King Avenue Columbus, Ohio 43201*

Received November 17, 1983
Accepted for Publication April 20, 1984

Creep rupture studies on five well-characterized Zircaloy-clad pressurized water reactor spent fuel rods, which were pressurized to a hoop stress of ~145 MPa, were conducted for up to 2101 h at 323°C. The conditions were chosen for limited annealing of in-reactor irradiation hardening. No cladding breaches occurred, although significant hydride agglomeration and reorientation took place in rods that cooled under stress. Observations are interpreted in terms of a conservatively modified Larson-Miller curve to provide a lower bound on permissible maximum dry-storage temperatures, assuming creep rupture as the life-limiting mechanism. If hydride reorientation can be ruled out during dry storage, 305°C is a conservative lower bound, based on the creep-rupture mechanism, for the maximum storage temperature of rods with irradiation-hardened cladding to ensure a 100-yr cladding lifetime in an inert atmosphere. An oxidizing atmosphere reduced the lower bound on the maximum permissible storage temperature by ~5°C. While this lower bound is based on whole-rod data, other types of data on spent fuel behavior in dry storage might support a higher limit. This isothermal temperature limit does not take credit for the decreasing rod temperature during dry storage. High-temperature tests based on creep rupture as the limiting mechanism indicate that storage at temperatures between 400 and 440°C may be feasible for rods that are annealed.

INTRODUCTION

Interim dry storage is being considered in the United States for light water reactor (LWR) spent fuel. Since the major sources of radioactivity generated in-reactor (actinides and fission products) reside in the pellet and fuel/cladding gap, it is desirable to preserve the cladding as an intact barrier during the storage period by limiting the storage temperature and specifying a storage atmosphere that minimizes cladding degradation.

The cladding can degrade either by external oxidation or in response to internal fuel rod conditions. Blackburn et al.[1] evaluated a number of these internal degradation mechanisms and identified stress rupture and stress corrosion cracking (SCC) as the most likely potential causes of cladding breach. Although cladding stress results primarily from rod prepressurization during manufacture, it is also normally increased a nominal amount by fission gas release from the fuel pellet. Since both stress rupture and SCC are thermally activated, it should be possible to limit cladding degradation by limiting the maximum cladding temperature for dry storage. Blackburn et al.[1] conservatively estimated a maximum permissible isothermal temperature of 304°C for a 1000-yr cladding lifetime relative to creep rupture and a peak temperature of 380°C if a time-dependent monotonically dropping temperature were taken into account. These temperature limits, however, are dependent on the validity of the underlying assumptions that involve the breach mechanisms, as well as the cladding material properties and physical condition. These temperature limits cannot be verified in a laboratory time frame; however, by accelerating potential degradation mechanisms with increased internal rod pressure or temperature

and using accepted creep rupture models, such as that of Larson and Miller,[2] confidence can be gained that the limits are conservative.

Since temperature was the easiest condition to vary experimentally (and also allowed the internal environment of the rod to remain undisturbed), a series of accelerated high-temperature tests was conducted on intact Zircaloy-clad pressurized water reactor (PWR) rods.[3] Blackburn et al.'s model[1] was used to determine test temperatures (480 to 570°C) at which cladding breaches should be obtained in a year or less. No breaches were obtained, and lifetime predictions were significantly exceeded. This resulted from a drop in cladding stress caused by cladding creep of up to 11%. A number of observations were made that might ultimately affect cladding lifetime:

1. There was no detectable release of fission gas.

2. Cracking of the external oxide layer occurred.

3. An oxygen-stabilized alpha Zircaloy layer formed between the cladding and the ZrO_2.

4. Cracks penetrated but were blunted in the oxygen-stabilized alpha Zircaloy.

5. Cladding creep was extensive.

When these observations were incorporated into the Blackburn et al. stress rupture model, a 100-yr cladding lifetime was predicted for intact spent fuel rods at storage temperatures as high as 440°C.[a]

The LWR Zircaloy fuel cladding is irradiation hardened with resulting changes in mechanical properties while in reactor. During the high-temperature tests, the irradiation hardening was annealed[4-6] so the cladding had material properties that were significantly different from those of irradiated cladding that never exceeded the annealing temperature in storage. For dry storage at temperatures above the irradiation-hardening annealing temperature, lifetime predictions based on the high-temperature tests and unirradiated creep-rupture properties probably adequately represent the cladding behavior. If the storage temperature does not exceed the annealing temperature, the cladding will remain in an irradiation-hardened state where the unirradiated properties may not satisfactorily represent the irradiated cladding properties. To determine the behavior of the cladding at lower long-term dry storage temperatures where irradiation hardening is largely preserved, a whole-rod test was conducted on overpressurized PWR rods at 323°C. This paper presents the results of that test and discusses the implication of these results on dry storage temperature limits.

[a]Reference 2 stated a 425°C temperature limit. Reevaluation of the data indicates that the temperature limit for 100-yr storage should be 440°C.

TECHNICAL APPROACH TO LIFETIME PREDICTION

Methodology

Larson and Miller[2] developed a formula to predict time to breach based on the creep rupture properties of a material and the applied stress. The formula can be used to obtain results under one set of test conditions in a laboratory time frame and relate those results to the expected behavior under a different set of conditions. A Larson-Miller parameter (LMP) was defined that related the temperature T to the breach time t_f:

$$\text{LMP} = T(\log t_f + 20) \ . \qquad (1)$$

The LMP can also be empirically related to the applied cladding hoop stress σ_H by the equation

$$\log \sigma_H = \sum_{i=0}^{3} a_i (\text{LMP})^i \ , \qquad (2)$$

where the coefficients a_i are determined by creep-rupture-type tests. When the coefficients a_i are known for a particular material, the lifetime t_f at temperature T can be determined for any applied stress σ_H by solving Eqs. (1) and (2). Since the Larson-Miller relationship should be written as

$$\text{LMP} = T \log[t_f + C(t)] \ ,$$

where $C(t)$ is a function of the material's creep (arbitrarily set at 20), the Larson-Miller relationship almost always predicts lifetimes shorter than actually observed in particular test cases.[7]

A typical LWR fuel rod stored at between 200 and 350°C would have a cladding hoop stress between 50 and 100 MPa. Results from high-temperature whole-rod tests[3] and supporting analyses[1] based on Larson-Miller coefficients for unirradiated Zircaloy indicate that the cladding stress rupture lifetime for this typical LWR rod should significantly exceed 1000 yr when the storage is in an inert atmosphere at temperatures below 350°C. Limitations on test temperature, pressure, and time (see the section on "Experimental Procedure" and Fig. 1) indicate that it may be difficult to find a set of test conditions that will accelerate cladding degradation sufficiently to confirm the predicted cladding lifetimes based on the creep-rupture properties of unirradiated Zircaloy. In any case, at temperatures below ~310°C, the cladding will remain in an irradiation-hardened state during storage so that the unirradiated Larson-Miller correlation may not be suitable.

As can be seen from Fig. 1, the majority of the anticipated dry storage conditions, in order to provide a 100-yr lifetime especially at temperatures below 310°C where the cladding will remain in an irradiation-hardened state, do not require creep rupture properties as good as indicated by the unirradiated creep-rupture curve. If we assume that the

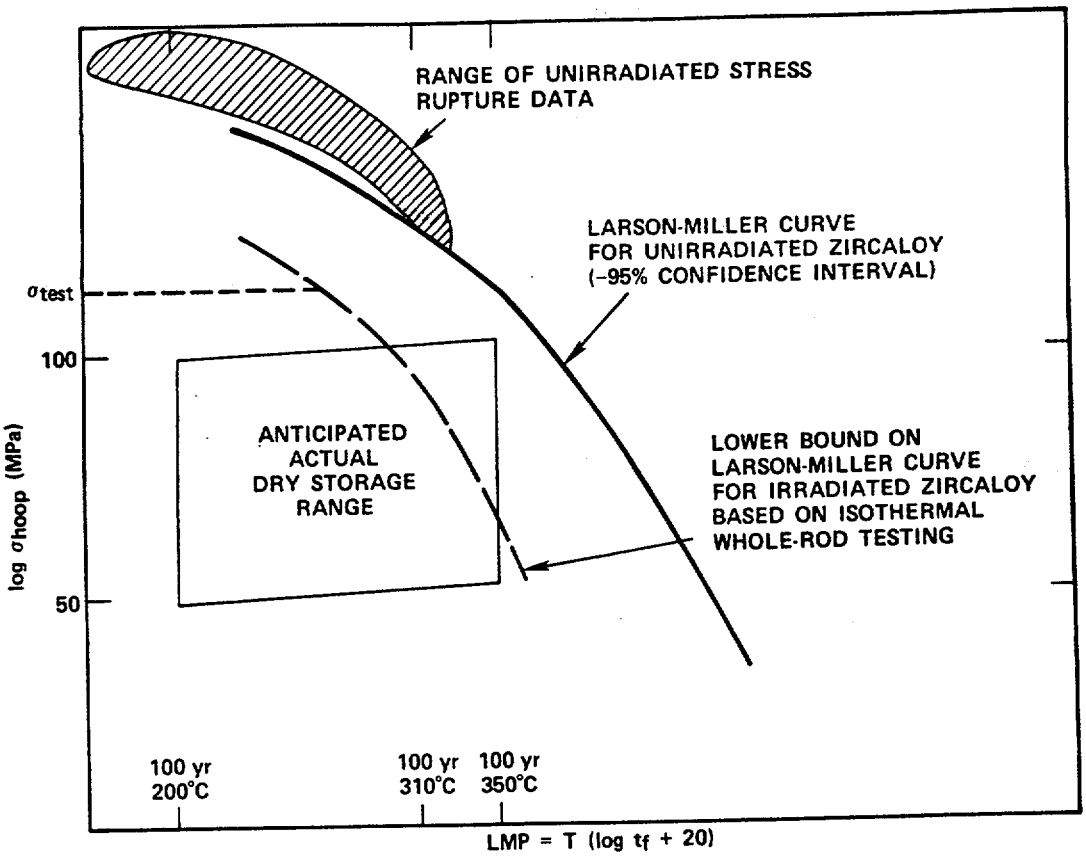

Fig. 1. Larson-Miller relationship for unirradiated Zircaloy.

Larson-Miller curve for irradiated Zircaloy has the same form as that for unirradiated Zircaloy and that the standard deviations in creep-rupture data for both irradiated and unirradiated Zircaloy are approximately the same, then we may be able to experimentally establish a lower bound on the irradiated creep-rupture properties by shifting the unirradiated Larson-Miller curve. This "shifted" curve is used to determine a lower bound in the maximum permissible storage temperature for cladding that remains in an irradiation-hardened state throughout its storage lifetime. Such a shift is illustrated in Fig. 1.

The magnitude of the shift is experimentally determined. Since a storage lifetime of at least 100 yr is desired and short duration tests are practical, test conditions must be set to accelerate the creep-rupture degradation of the cladding. Equations (1) and (2) predict a shortened lifetime if the hoop stress is raised. If no breach occurs during the test at the elevated stress, Eqs. (1) and (2), which are based on the Larson-Miller curve for unirradiated Zircaloy, are adjusted to predict breach for the test duration. This forms a lower bound on the actual Larson-Miller curve for irradiated Zircaloy than if the creep-rupture properties of irradiated Zircaloy had been available. This adjusted or "shifted" curve is then used to predict lower bounds on lifetimes on temperatures under actual storage conditions.

If one assumes the test rod has better creep-rupture properties than 95% of the general population of LWR rods, the LMP can be calculated for the test from the equation

$$\log \sigma_t(T_t) = \sum_{i=0}^{3} a_i^{+95} [\mathrm{LMP}_{+95}(T_t)]^i \ , \qquad (3)$$

where $\sigma_t(T_t)$ is the hoop stress in the cladding at test temperature T_t and a_i^{+95} are the material creep-rupture coefficients applicable to the +95% confidence interval for unirradiated Zircaloy. The time to breach t_f for a rod having a cladding stress $\sigma_t(T_t)$ is given by the equation

$$\mathrm{LMP}_{+95}(T_t) = T_t(\log t_f + 20) \ , \qquad (4)$$

where $\mathrm{LMP}_{+95}(T_t)$ is calculated from Eq. (3). It was assumed that if coefficients a_i suitable for irradiation-hardened Zircaloy had been used in Eq. 3, the test would have terminated at t_t with a cladding breach. Therefore,

$$t_f = \alpha t_t \ . \qquad (5)$$

The factor α determines the extent of the shift in the Larson-Miller creep-rupture curve in order that test

data can be used to make conservative bounding lifetime predictions for irradiated rods. By sequentially determining $LMP_{+95}(T_i)$ from Eq. (3) and t_f from Eq. (4), α can be calculated from Eq. (5). Under actual storage conditions, minimum lifetimes (t_M) can be calculated as a function of storage temperature (T_s) using the equations

$$LMP_{-95}(T_s) = T_s(\log \alpha t_M + 20) \quad (6a)$$

and

$$\log \sigma_s(T_s) = \sum_{i=0}^{3} a_i^{-95}[LMP_{-95}(T_s)]^i , \quad (6b)$$

where $\sigma_s(T)$ is the cladding hoop stress at T_s and a_i^{-95} are the −95% confidence level creep-rupture coefficients. The −95% coefficients are used in order to predict the behavior of the poorer rods in the general population.

Storage Cladding Hoop Stress

Fuel rods will undergo cladding creep,[3] cladding oxidation, and crack propagation[3] during storage. Using the thin wall hoop stress relationship, a 2:1 biaxial stress state since the stress is caused by gas pressure, treating the He-10% Xe mixture as an ideal gas, and accounting for all three of the above phenomena, the instantaneous cladding hoop stress is given by

$$\sigma_H = \frac{PT}{592} \times \frac{V_{23}}{V_T} \times \frac{D_o(1+\epsilon) - H(1-\epsilon) + 2W + O_2}{h(1-\epsilon) - 2W - O_2} , \quad (7)$$

where

P = internal pressure at 23°C (MPa)

ϵ = creep strain (mm/mm)

V_i = internal rod volume at test temperature (m^3)

V_{23} = internal rod volume at room temperature (m^3)

T = storage temperature (K)

D_o = outside diameter (mm)

h = initial wall thickness (mm)

W = crack depth (mm)

O_2 = total external oxide thickness (mm) (see Fig. 2)

t = time (yr).

The crack depth W is given by

$$W = 2.21 \times 10^4 \left[t \exp\left(\frac{-22\,910}{T}\right)\right]^{+1/2} , \quad (8)$$

which was developed on the basis of the high-temperature whole-rod studies.[3] The oxide thickness

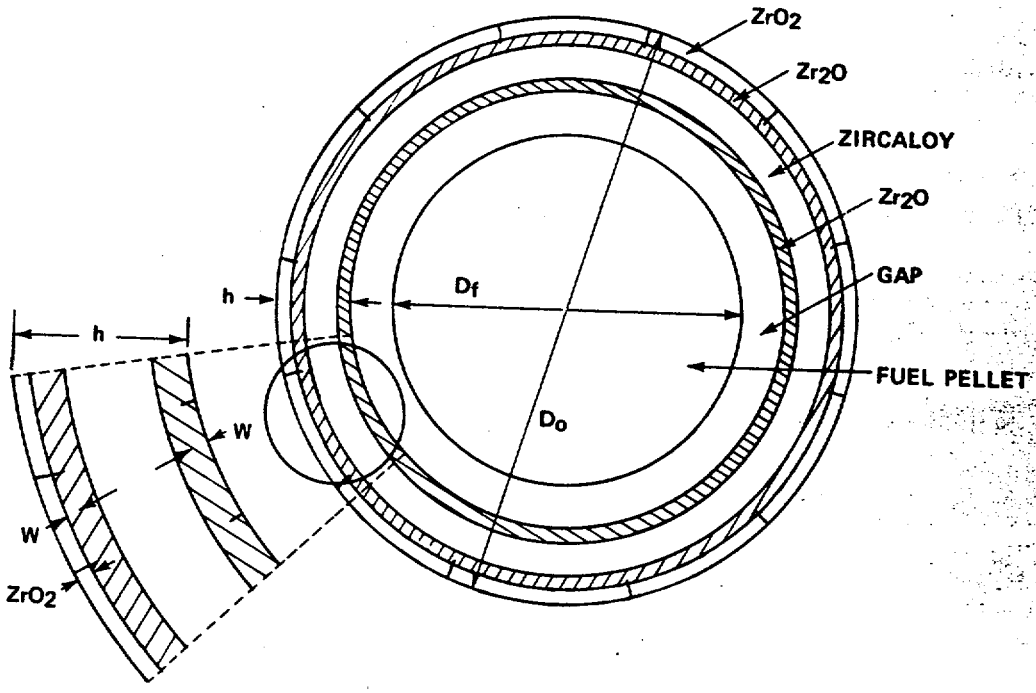

Fig. 2. Schematic cross section of fuel rod.

O_2, based on posttransition kinetics, is time-and-temperature dependent[8]:

$$O_2(\text{mm}) = 3.68 \times 10^8 \times t \times \exp\left[\frac{-15\,810}{T(\text{K})}\right] . \quad (9)$$

Equations (7), (8), and (9) taken together give a time-and-temperature-dependent description of the cladding hoop stress during storage.

The extent to which cladding will oxidize during storage below 350°C is based on extrapolation. Hillner's oxidation[8] studies in steam and Watson's studies[9] of Zircaloy-2 oxidation in air between 500 and 700°C both indicate that the rods should be in posttransition oxide growth by the time they enter dry storage. It is not known whether the oxide will continue to grow as posttransition oxide or revert to pretransition oxide growth rates at the lower storage temperatures. Since the oxide growth rate is faster in posttransition,[8,9] conservatism requires that posttransition rates be used to determine wastage. There have been many oxidation studies in water and steam, mostly at temperatures in excess of 500°C, but relatively few studies in a dry atmosphere (e.g., low humidity). The dry oxidation studies were also at temperatures above 500°C and were conducted for short time periods.[9] Boase and Vandergraaf[10] compared posttransition oxidation rate data above 500°C and found close agreement between oxidation in steam, water, and air; Eq. (9) is based on extrapolation of their data.

Equations (7), (8), and (9) describe a time-and-temperature-dependent hoop stress during storage. While rod stress can be calculated as a function of time if adequate low-temperature creep equations are available, lifetime predictions are uncertain under a varying stress since there is no proven method of adding cumulative damage. A number of simplifying assumptions were made so lifetimes could be calculated in terms of a constant cladding stress. All these assumptions are conservative and lead to a stress higher than expected in storage:

- *No cladding creep takes place during storage* ($\epsilon = 0$). It was shown in the high-temperature tests[3] that fuel rod geometry is such that internal rod pressure and, consequently, stress drop as cladding creep takes place. Due to the uncertainty in low-temperature creep rates,[11-15] the conservative position does not take credit for the stress reduction due to creep.

- *Isothermal storage* (T = constant). In reality, the fuel rod temperature drops due to a drop in the decay heat. Since stress is proportional to pressure which is proportional to temperature, if temperature drops, stress drops. In addition, according to Eqs. (8) and (9), both the oxidation and cracking wastage are thermally activated so that a drop in temperature reduces wastage.

- *A Westinghouse 15 × 15 assembly was considered as a base case* ($D_o = 10.72$ mm and $h = 0.61$ mm). In the as-fabricated state, D_o/h varies from a high of 17.54 for a rod from a Westinghouse 15 × 15 assembly to a low of 15.16 for a rod from a Combustion Engineering 16 × 16 assembly; hence, a rod from a Westinghouse 15 × 15 assembly is the most conservative case.

- *Cladding wastage due to oxidation and cracking are at end-of-storage period value for the complete storage duration* ($t = t_f$). This is a conservative position since cladding wastage is greatest at the end of storage. For example, during storage for 100 yr at 300°C, a 38-μm wastage is assumed from the beginning of storage even though it forms linearly with time according to Eq. (9). It has also been assumed that the cladding wastage is equal to oxide thickness. This is not true due to the differences in density of Zircaloy (6.49 g/cm^3) and ZrO_2 (5.6 g/cm^3 theoretical). Since the density rates can vary from 60 to 86% due to the ZrO_2 morphology, no credit has been taken for the difference in density.

The conservatism of these assumptions can be decreased or eliminated if validated methods can be developed to treat time-varying conditions.

EXPERIMENTAL PROCEDURE

Materials and Equipment Description

The tests were conducted in a shielded seven-zone furnace capable of holding seven individually encapsulated and modified PWR fuel rods. The capsules were placed around an instrument tree containing ten axially located Chromel-Alumel thermocouples. Details of the furnace construction are described elsewhere.[16]

Five Westinghouse-designed 15 × 15 prepressurized PWR rods from Turkey Point Unit 3 reactor were tested. The rods had been irradiated for two or three cycles of operation and discharged from the reactor ~6.6 yr prior to testing.[17-19] The cladding was fabricated from 10.72-mm-o.d., cold-worked, stress-relieved, annealed Zircaloy-4 tubing with a 0.62-mm wall thickness. The fuel column was composed of 2.6% enriched UO_2 fuel pellets that were 92% theoretically dense. The rods operated at ~18.7 kW/m with an average measured centerline burnup of 650 MWh/kgU for the two-cycle rods and 746 MWh/kgU for the three-cycle rods.[20]

Pretest Rod Characterization

Test controls or reference conditions were established by nondestructive examinations on all test rods and by destructive examinations on companion rods from the same assemblies. The rods were visually examined for crud accumulation and gross defects. Diameters were measured using helical profilometry, and both ^{137}Cs and total fission product distributions were determined by gamma scanning. The destructive examinations included measurements of internal pressure, fission gas content, surface oxidation, hydride distribution, fuel structure, and cladding corrosion. Results of pretest examinations and details of the examination techniques have been reported previously.[17,20]

Test Conditions and Procedures

To apply the analyses described in the section on the "Technical Approach to Lifetime Prediction" to rods stored at temperatures where irradiation hardening does not anneal, it was necessary to set test conditions so that (a) the test rod cladding was under a nearly constant stress, (b) no significant annealing of the test rod cladding would occur, and (c) no extraneous breach mechanisms would be introduced. The threshold stress for short-term SCC at a temperature of 300 to 350°C appears to be between 152 and 200 MPa (Refs. 21 and 22). Since a maximum hoop stress of 90 MPa is expected[23] during storage and SCC may not be a problem,[24] an upper limit of 152 MPa was placed on the cladding stress at temperature in order not to artificially induce SCC during the test. A creep strain of 2×10^{-4} is required to reduce the cladding stress ~1% when the volume occupied by the fuel pellet is considered. At 152 MPa, preliminary analysis (described in the section on lifetime prediction) indicates that the most significant data occur in the first 2000 to 4000 h of the test. Based on a 6-month test and a maximum stress decrease during the test of 1.5%, the creep-strain rate was limited to ~10^{-7}/h. Available creep data range over two orders of magnitude for any given stress level and temperature.[17] The highest rates[17] were used to determine an upper test temperature of 325°C. When measurements of irradiation recovery in Zircaloy, taken for <100 h (Refs. 4 and 5) are extrapolated to 4000 h, recovery was expected to be between 0 and 40% during the test period. Therefore, the test was run for 2101 h at 323°C using rods pressurized to a cladding hoop stress of ~152 MPa at temperature.

The test rods were modified so that a 152-MPa cladding stress could be obtained while preserving the internal environment. The fission gas and helium were released into a vacuum through a hole drilled in the top end cap, and the rod was backfilled with helium. A second end cap, consisting of a stainless steel tube brazed into a Zircaloy adaptor, was welded onto the rod under an argon stream. The rod was evacuated, then backfilled with a He + 10% Xe mixture to either 9.2 or 9.5 ± 0.2 MPa at room temperature (see Table I). The rods were sealed by cold-welding the stainless steel tube and then helium-leak checking to a leak rate no larger than 1×10^{-9} std cm^3/s at 23°C. Each rod was placed in an individual capsule that was filled with either 0.1 MPa argon or 0.25 MPa air at room temperature. Based on posttransition oxidation rates of Zircaloy,[8-10] the air pressure in the sealed capsules was chosen to simulate unlimited air that would not be depleted to less than 10% O_2. The capsule pressure was monitored continuously to detect any pressure rise indicative of a gas leak from the fuel rod.

TABLE I

Capsule Atmospheres and Internal Rod Pressures

Rod	Test Time (h)							
	0 to 31		31 to 231		231 to 1769		1769 to 2101	
	Internal Pressure[a] (MPa)	Atmosphere	Internal Pressure[a] (MPa)	Atmosphere	Internal Pressure[a] (MPa)	Atmosphere	Internal Pressure[a] (MPa)	Atmosphere
TPDO4-I9	9.2	Argon	9.2	Air	9.2	Air	<0.5	Argon
TPB17-G6	9.5	Air	<0.5	Argon	<0.5	Argon	<0.5	Argon
TPB17-I6	9.2	Argon	9.2	Argon	<0.5	Argon	<0.5	Argon
TPDO4-H6	9.2	Argon	9.2	Argon	9.2	Argon	9.2	Argon
TPDO4-I6	9.5	Air	9.5	Air	9.5	Air	<0.5	Argon

[a]At room temperature.

RESULTS

Operating Experience

The rods were brought to the test temperature of 323 ± 2°C at a rate of <50°C/h. The temperature variation at any one location during the test did not exceed ±6°C with the axial temperature profile shown in Fig. 3. The test ran continuously at 323 ± 2°C for 2101 h, except for power outages that shut the test down at 31, 231, and 1729 h. The heatup and cooldown periods were not counted when determining the time at temperature. As the furnace cooled to ~200°C, one rod released its internal gas pressure during each of the first two outages, and two rods released their gas during the third outage (see Table II). The rate of cooldown during the power outages was <20°C/h. In order to preserve the integrity of the fifth rod, the test was terminated with a controlled cooldown rate of 5°C/h.

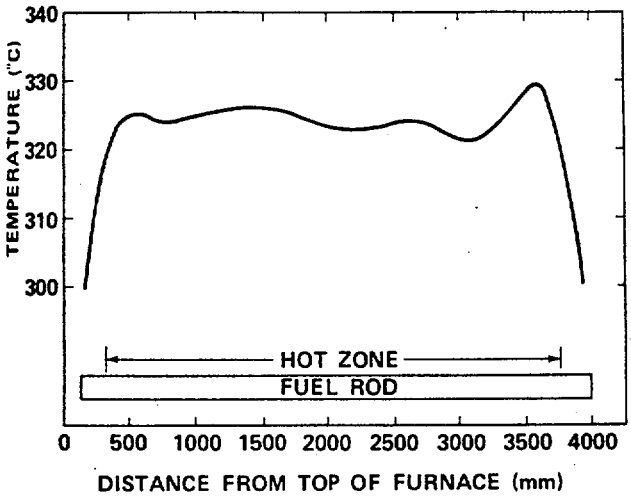

Fig. 3. Axial temperature profile in the furnace.

During the test, the cause of the rod breaches was unknown. Due to furnace and hot cell logistics, it was impractical to remove and examine the rods during the shutdown in which the rods breached. To preserve the breach characteristics until posttest examinations could be conducted, the capsules in which breaches occurred were backfilled with argon during the shutdown in which they breached. The breaches were later determined to be at the braze around the capsule fill tube and not in the cladding.

Fuel Rod Performance

Nondestructive Examination

After the test, each rod was visually examined, profiled, and both gross and ^{137}Cs gamma scanned. There was no visible degradation of the rod. The gamma scans indicated no fuel or fission product redistribution, which is consistent with observations from the 482°C test.[3] The four rods (see Table III) that breached at the end fittings before the end of the test had very little or no cladding strain over the length of the rod; the measured strain was less than the measurement error of 0.07%. This was expected since the internal rod pressures were set so that essentially no cladding strain would be expected to occur during the test. Rod TPDO4-H6, which operated 2101 h under pressure, had an average cladding strain over the length of the rod of 0.16%. This corresponds to an ~8% drop in cladding hoop stress.

Destructive Examination

A destructive examination was conducted on the three rods indicated in Table IV. Transverse metallography samples were taken from the fuel midplane (i.e., 1829 mm from the fuel bottom) and at the location of the maximum pretest hydride concentration (3100 mm from the fuel bottom). The results of the examination are given in Table IV. While the external oxide thickness did vary axially, there was no increase in thickness

TABLE II

Test Conditions

Rod	Time at Test Temperature and Pressure (h)	Time Test Temperature After Loss of Rod Pressure (h)	Number of Cooldown Cycles	Last Pressurized Cooldown Rate (°C/h)
TPDO4-I9	1769	332	3	9.4
TPB17-G6	31	2070	1	14.3
TPB17-I6	231	1870	2	10.3
TPDO4-H6	2101	0	4	5
TPDO4-I6	1769	332	3	9.4

TABLE III

Cladding Stress and Creep Strain

Rod	Time at Test Temperature[a] and Pressure (h)	Capsule Pressure (MPa) at Room Temperature	Internal Rod Pressure (MPa) at Room Temperature	Average Rod Stress (MPa) at 323°C	Initial Rod Outer Diameter (mm)	Average Cladding Creep (%)
TPDO4-I9	1769	0.24	9.25	150 ± 3	10.69 ± 0.01	0.004 ± 0.02
TPB17-G6	31	0.26	9.52	152 ± 3	10.67 ± 0.02	−0.005 ± 0.08
TPB17-I6	231	0.11	9.25	152 ± 3	10.64 ± 0.02	0.053 ± 0.07
TPDO4-H6	2101	0.12	9.25	146 ± 3	10.68 ± 0.02	0.157 ± 0.06
TPDO4-I6	1769	0.25	9.52	157 ± 3	10.69 ± 0.01	0.02 ± 0.03

[a]All rods were at 323°C for a total time of 2101 h. 87 days

TABLE IV

Posttest Cladding and Gap Characteristics

Rod	Average Cladding Thickness (μm)	Average Oxide Thickness (μm)		Radial Oxide Cracking		Fuel/Cladding Gap (μm)	Fuel/Cladding Chemical Interaction Inner Diameter Coverage (%)
		Distance from Bottom of Rod (mm)					
		1830	3100	1830	3100		
TPB17-G6	630 ± 13	5 ± 2	17 ± 4	No	No	19 ± 12	37
TPDO4-H6	622 ± 20	6 ± 1	13 ± 3	Yes	No	48 ± 27	0
TPDO4-I6	613 ± 8	7 ± 1	14 ± 3	No	Yes	34 ± 8	12
DO4-pretest (Refs. 13 and 15)	625 ± 8	5 ± 1	---			50 ± 25	
B17-pretest (Refs. 13 and 15)	622 ± 8	6 ± 2	15 ± 5			38 ± 13	

from pretest values. This would be expected due to the short test time and low temperature [Eq. (9) predicts a 0.25-μm oxide growth]. The rods that were under pressure for 1760 h or longer exhibited equispaced radial cracks in the external oxide layer. A similar effect was found on the rods that underwent creep in the high-temperature whole-rod test.[2] The cladding thickness and fuel/cladding gap did not measurably change during the test. This would also be expected since there was no measurable cladding oxidation, and minimal creep was detected in only one rod.

Cladding hardness was used to monitor the irradiation-hardening recovery. Five equispaced indents, using a 0.2-kg weight, were taken along four cladding radii on each metallographic sample. As shown in Fig. 4, within measurement error, the cladding hardness after 2100 h at 323°C was essentially the same as when the cladding was removed from the reactor; this indicates that there was no annealing of the irradiation hardening. This behavior can be compared to the large drop in cladding hardness seen in the 482 and 571°C tests, indicating significant annealing. Although there is some inconsistency in the irradiation-hardening annealing data[4-6] (see Fig. 5), probably due to differences in irradiation temperature, the lack of annealing in the present test was expected.

Cladding samples immediately adjacent to the metallographic samples were analyzed for hydrogen content using the inert gas fusion technique. No increased hydrogen pickup or axial hydrogen migration was indicated (see Table V). This is not unexpected since the rod tested between 482 and 571°C for longer periods of time also showed no pickup or axial migration.[3]

The as-irradiated cladding had a random distribution of small circumferential hydrides as a result of the

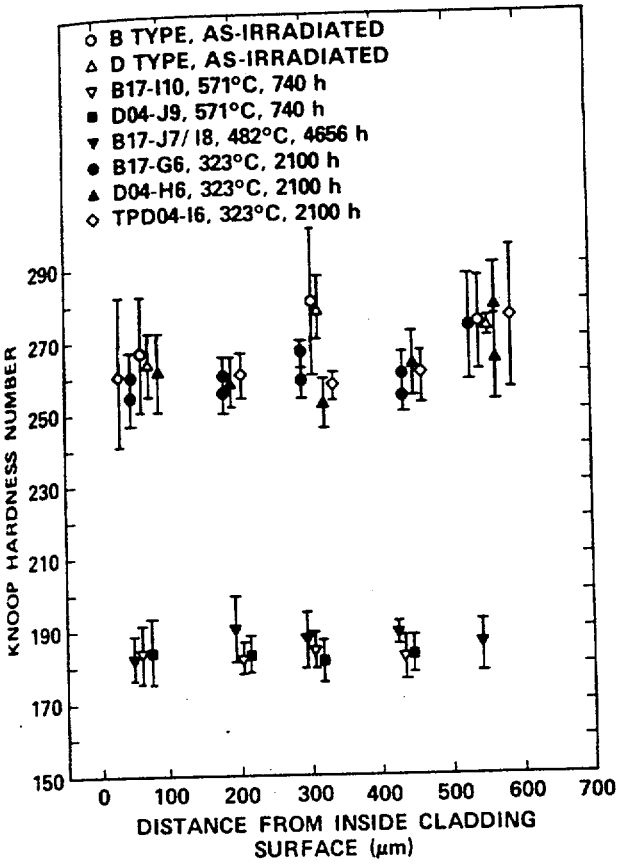

Fig. 4. Comparison of pre- and posttest hardness measurements.

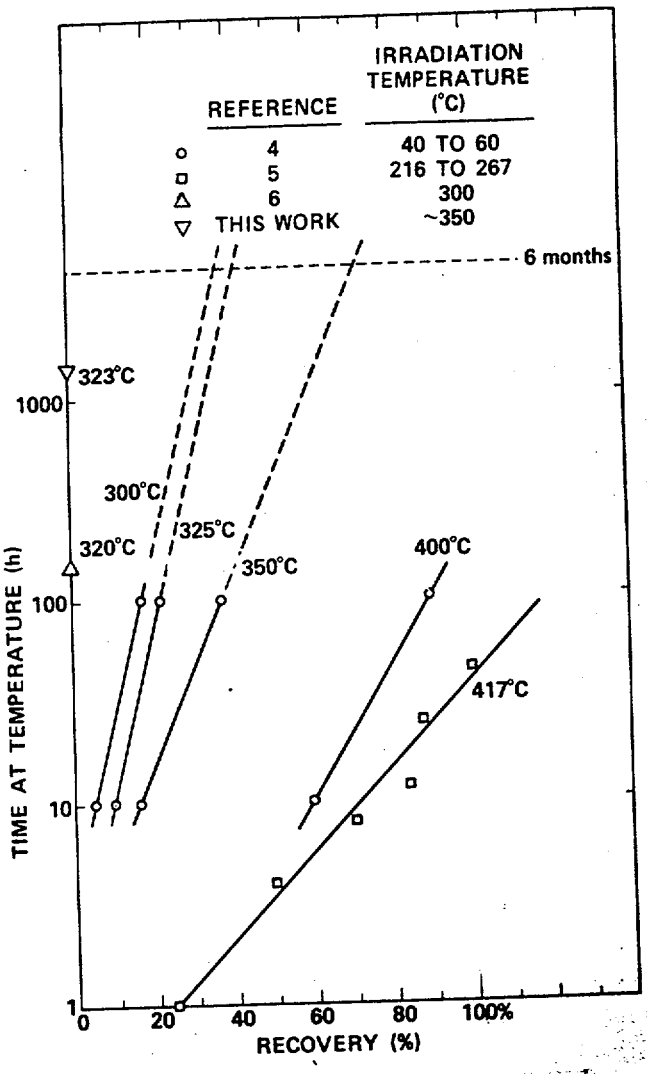

Fig. 5. Irradiation damage recovery in Zircaloy.

fabrication steps used to control the Zircaloy texture.[25] After this test (see Figs. 6 and 7), the hydrides' radial location in the cladding, density, size, and orientation are dependent on the axial location in the rod and the time at temperature since the last cooldown under pressure. At the 1800-mm elevation (where the hydrogen content is ~30 ppm), small hydrides were precipitated during cooldown near the inner and outer cladding surfaces. Generally, the central region of the cladding is denuded of hydrides. The rod that released its pressurization gas at 31 h and thus had 2070 h at 323°C with no internal pressurization or cladding stress exhibited circumferential hydrides near both surfaces. With only 332 h at 323°C and no internal pressurization or cladding stress, the hydrides on the inner cladding surface are in part radially oriented. Most of the hydrides on both surfaces of the rod that maintained an internal gas pressure and cladding stress for the total time at temperature as well as during cooldown were radially oriented. This was not unexpected since hydrides precipitating under stress tend to align nearly perpendicular to the tensile stress axis in polycrystalline specimens.[26] In the present case, the hoop stress is in the circumferential direction, so the hydrides are in a radial direction. After the stress is removed, the hydrides go back into solution when the rod is heated and then precipitate in the circumferential direction when there is no stress during cooldown(s).

At the 3100-mm fuel rod elevation (where the hydrogen content is ~90 ppm), hydride reorientation is similar to that seen at the lower elevation. However, as a result of the higher hydrogen content, no denuded zone is observed in the center of the cladding and there are more and larger hydrides. There are regions where radial hydrides nearly extend across the complete wall thickness. This behavior is significantly different from that observed in the high-temperature whole-rod tests,[3] where the rods cooled at ~10°C/h under much lower hoop stress and all observed hydrides were circumferentially oriented.

TABLE V

Cladding Hydride and Hydrogen Characteristics

Rod	Elevation from Bottom of Rod (mm)	H_2 Content (ppm)	Hydride Orientation[a]	Time at Temperature After Last Pressurized Cooldown (h)
DO4-H6	1813	31 ± 6	Inner/outer 25%-mixed R/C	0
	3083	86 ± 6	Predominantly R, some C	0
DO4-I6	1813	30 ± 6	Inner, 25% C; outer, 10% C	332
	3083	97 ± 5	Predominantly C, some R	332
B17-G6	1813	32 ± 7	Inner, C; outer, C	2070
	3083	90 ± 6	All C	2070
Pretest	1813	50 ± 15	Uniformly distributed small C	---
	3083	100 ± 10	Uniformly distributed small C	---

[a]C = circumferential; R = radial.

Rod Hoop Stress During Test

While the rods were initially pressurized to give a nominal stress of 152 MPa, the actual cladding stress for the start and end of the test was calculated using measured dimensions of the rods where possible. Equations (8) and (9) predict that the cladding cracking and oxidation should not exceed 0.1 and 0.25 μm, respectively, for 2101 h. Posttest examination confirmed this; neither cracking nor additional cladding oxidation was observed. As a result, Eq. (7) can be reduced to

$$\sigma_H = \frac{PT}{592} \times \frac{V_{23}}{V_T} \frac{D_o - h}{h} \quad . \qquad (10)$$

Using a room temperature internal rod-free volume of 22.8 ± 1.0 ml (Refs. 13 and 15) and coefficients of thermal expansion $\alpha_{Zr(axial)} = 1.37 \times 10^{-6}$ m/m·°C^{-1}, $\alpha_{Zr(diam)} = 2.07 \times 10^{-6}$ m/m·°C^{-1}, and $\alpha_{UO_2} = 2.77 \times 10^{-6}$ m/m·°C^{-1} (Ref. 27), an internal volume decrease due to a thermal expansion (V_T/V_{23}) of ~0.97 was calculated. For two rods, 2 and 8% volume increase corrections at the end of the test were added to account for the cladding creep. With these corrections, the average of the beginning and end of test stresses is given in Table III.

DISCUSSION OF RESULTS

Maximum Permissible Storage Temperatures

There is little latitude to vary test conditions without annealing the irradiation hardening or introducing extraneous breach mechanisms. The test conditions were set to accelerate the creep-rupture mechanism and make use of the Larson-Miller formalization modified in the section on lifetime prediction to determine a lower bound for the maximum permissible storage temperature.

The 95% confidence interval LMP for 323°C and the test conditions are found from Eq. (3) using the actual test times at temperature and pressure, the lower tolerance on the average stress (given in Table III), and the material creep-rupture coefficients for unirradiated Zircaloy developed by Blackburn et al.[1] This LMP was then used in a combination of Eqs. (4) and (5) to determine α, which ranges from 1.4×10^5 for rod TPDO4-I6 to 1×10^7 for rod TPB17-G6. For any given internal rod pressure and desired lifetime, Eqs. (6a) and (6b) can be solved to determine a lower bound for the maximum permissible storage temperature. Alternatively, Eqs. (6a) and (6b) can be solved graphically (as shown in Fig. 8).

Figure 8 shows a solution for a 100-yr storage lifetime t_M with three internal rod pressures and two storage atmospheres. The lines labeled with rod numbers are plots of Eq. (6a) using α obtained for that particular rod. The curves labeled with rod pressures and atmospheres are the plots of Eq. (6b) when Eqs. (7), (8), and (9) are used for the stress along with the simplifying assumptions. The solutions to Eqs. (6a) and (6b) are given by the intersection of the two sets of curves. Consider, for example, the 2.07-MPa pressure curves. In general, the longer the rod operated under accelerating test conditions, the higher the lower bound on the maximum permissible storage temperature under storage conditions. All five rods operated for at least 30 h, which indicates a lower bound on the maximum permissible storage temperature of 295°C.

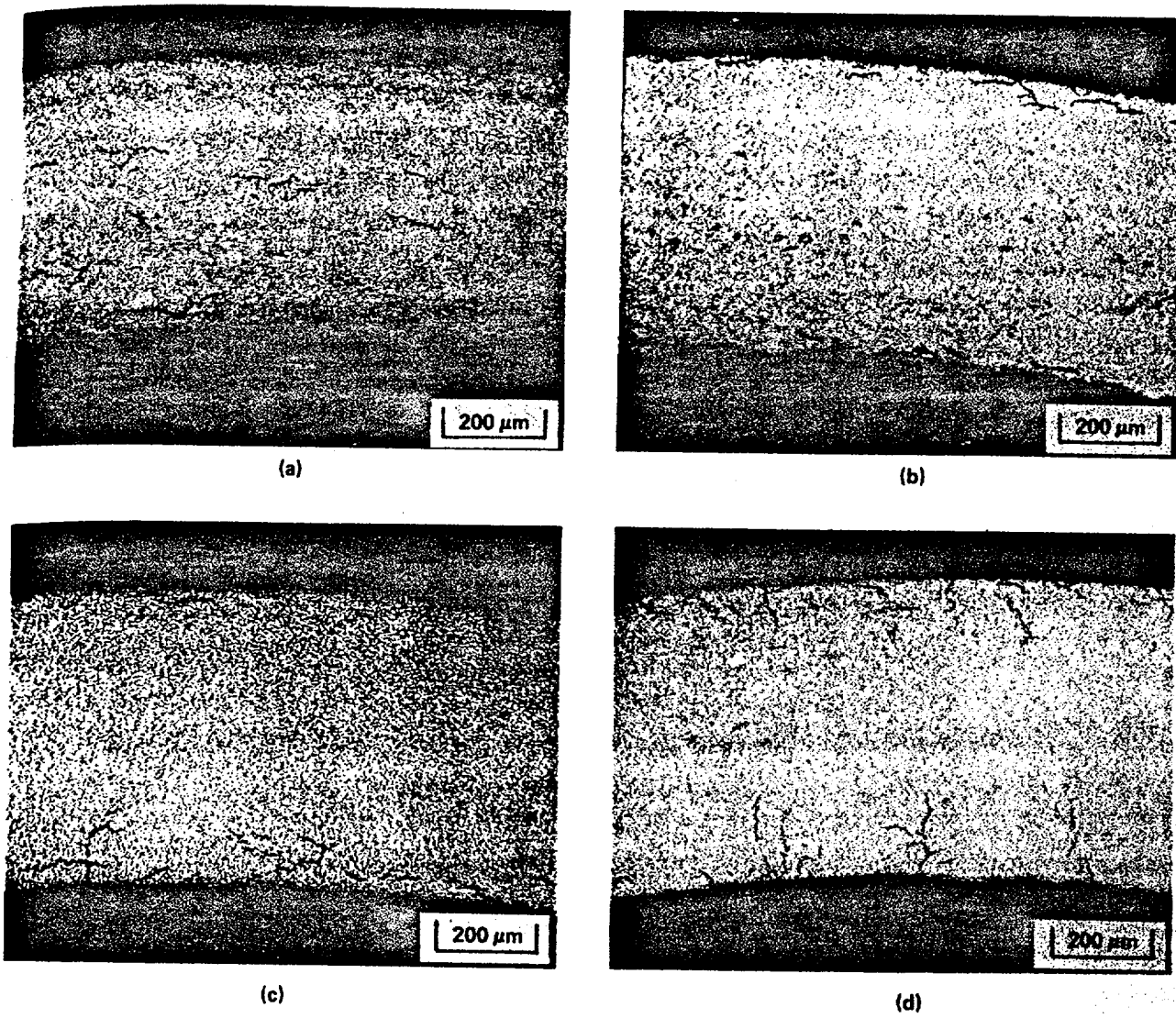

Fig. 6. Hydride precipitation at 1800-mm elevation (a) as-irradiated, (b) 2070 h at 323°C after pressurized cooldown, (c) 332 h at 323°C after pressurized cooldown, and (d) zero hours at 323°C after pressurized cooldown.

(intersection 1). One rod, TPDO4-I6, indicates a lower temperature bound of 328°C for the maximum permissible storage temperature (intersection 2), but this was not the rod that operated for 2100 h. The stress in rod TPDO4-H6 (intersection 3) dropped due to a cladding creep, so the accelerating force was not as large as for the other rods. Therefore, the added test time did not translate to a higher storage temperature. Three rods operated for 1729 h under test conditions before being suspended, so intersection 3 was used to establish the lower bound for the maximum permissible storage temperature. The lower bound for the maximum permissible storage temperature for rods that have not undergone cladding annealing is shown in Fig. 9 as a function of internal rod pressure for a range of desired lifetimes. In general, as the internal rod pressure drops or the desired lifetime goes down, the lower bound for the maximum permissible temperature rises.

The validity of the extrapolations to long storage times based on short-term high-stress tests is dependent on three items:

1. accuracy of the stress during the test, which was discussed earlier
2. conservatism of the stress anticipated under actual storage conditions
3. validity of the use of the Larson-Miller method with a shifted creep-rupture curve.

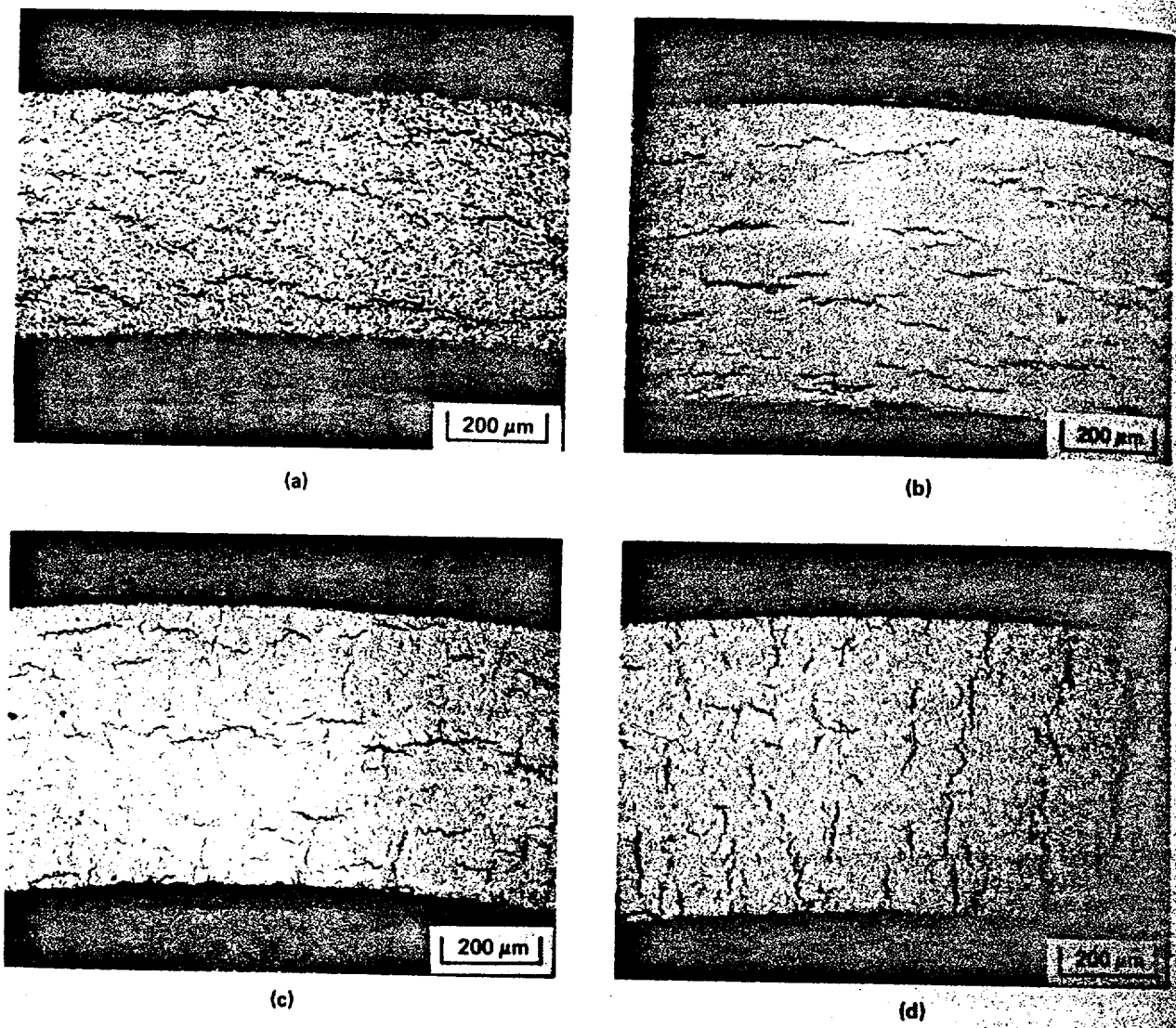

Fig. 7. Hydride precipitation at 3100-mm elevation (a) as-irradiated, (b) 2070 h at 323°C after pressurized cooldown, (c) 332 h at 323°C after pressurized cooldown, and (d) zero hours at 323°C after pressurized cooldown.

Table VI gives the percentage of cladding assumed to be wasted due to cracking and oxidation at the isothermal storage temperature. The maximum conservatism on the temperature limits due to an overstatement of the wastage (and hence storage stress) is the difference in the temperature limit when the wastage is considered and when there is no wastage. This conservatism is also tabulated in Table VI. Minimal cracking occurs at these storage times and temperatures; therefore, no temperature conservatism is gained. For an oxidizing atmosphere, there is an appreciable conservatism for longer storage periods, but for 100-yr storage, the conservatism is minimal. There may be a conservatism due to the shift of the Larson-Miller creep-rupture curve as represented by the alpha factor. Alpha, which is generated from the test data, represents the shift in the unirradiated creep-rupture curve that would be necessary to predict breach at the end of the test duration for test conditions. For rods DO4-I9 and DO4-H6, which were used to determine storage temperatures, alpha was $\sim 1.8 \times 10^5$. If the test rods had breached, then there would be no conservatism due to the shift of the Larson-Miller curve. The fact that breach did not occur and metallography gave no indication of cladding degradation implies that some undetermined amount of alpha must be due to a conservatism placed on the creep-rupture properties of irradiation-hardened Zircaloy.

The results of the whole-rod tests are summarized in Fig. 10. The high-temperature data[3] are all at temperatures where the annealing of the irradiation hardening of the cladding has been accomplished very

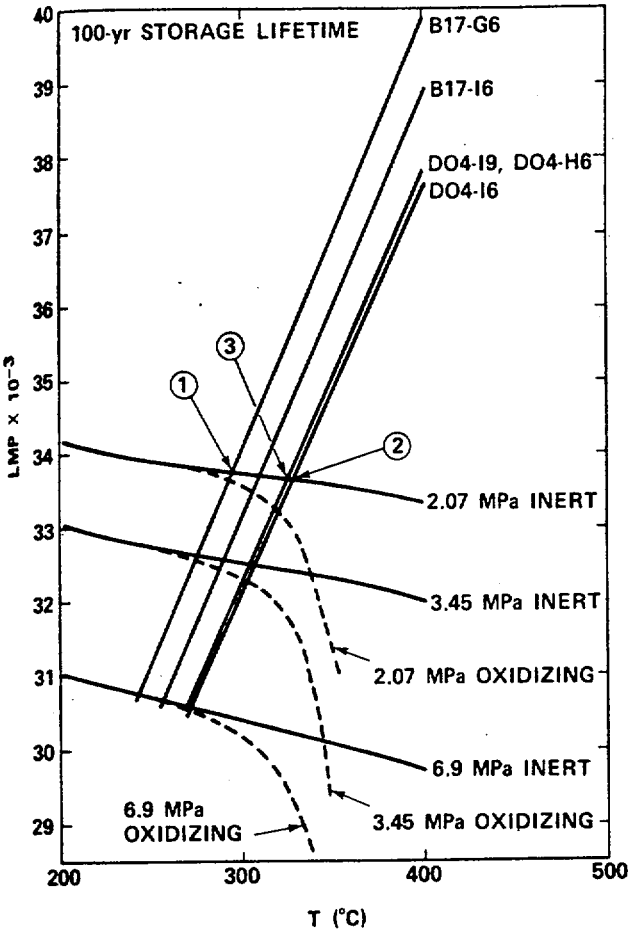

Fig. 8. Determination of lower bounds for the maximum permissible storage temperature by solution of Eqs. (6a) and (6b) for 100-yr storage lifetime. Lines labeled with rod numbers are plots to Eq. (6a) using α determined by the indicated rod. Curves labeled with pressures and atmospheres are plots to Eq. (6b) for the indicated conditions. Intersections 1, 2, and 3 refer to three solution cases discussed in the text.

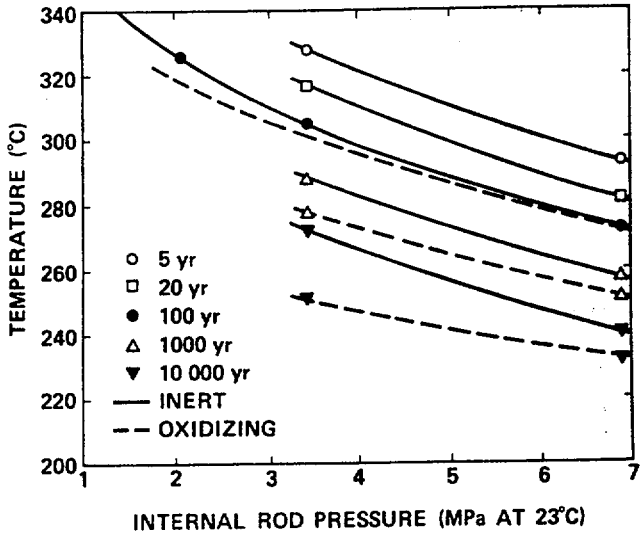

Fig. 9. A lower bound for the maximum permissible storage temperature based on the creep-rupture mechanism for rods that did not undergo annealing of the irradiation hardening.

rapidly and the low-temperature data are in a temperature range where no annealing of the irradiation hardening has taken place. The two sets of data can be used to predict lower bounds on the maximum permissible temperature as long as the condition of the cladding during storage is the same as the condition of the cladding during testing. These two sets of data do not form a complete data base since, as indicated in Fig. 10, there is an ill-defined temperature range where the cladding will be in a partially annealed state that will be constantly changing with time until 100% annealing occurs. In this temperature range one might expect cladding lifetimes to be longer than those predicted by the irradiation-hardened cladding lifetime curve and shorter than those predicted by the annealed cladding lifetime curve; however, there is currently not enough whole-rod test data or information concerning the addition of cumulative damage to allow a time/temperature lifetime curve based on the creep-rupture mechanism to be determined for partially annealed cladding.

Hydride Reorientation

After rod DO4-H6 cooled under stress (145 MPa at 323°C), the hydrides were oriented predominantly in the radial direction (see Figs. 6 and 7), while rod B17-G6, which cooled with no cladding hoop stress, had only circumferentially oriented hydrides. Between these two stress extremes are rods from the high-temperature whole-rod test (13 to 26 MPa), which showed no reorientation of the hydrides[3] although there was some agglomeration due to the slow cooling rate,[28] and standard reactor shutdown rods (50 MPa compressive), which also exhibited no reorientation of hydrides. Spent fuel rods with 2 to 7 MPa internal pressure at room temperature will have cladding stresses in the stress range bounded by these examples.

Hydrogen levels in PWR rods generally range from 40 to 100 ppm. Marshall and Louthan[29] have shown that when the concentration of hydrides oriented perpendicular to the stress vectors exceeds 40 ppm there is a severe degradation of the Zircaloy mechanical properties. Ductility drops[25,30] with increased radial hydrides[29] and tubes tend to breach at lower stresses. When the solubility limit is exceeded

TABLE VI

Temperature Conservatism Due to Assumptions on Cladding Wastage

Storage Time (yr)	Storage Temperature (°C)		Cladding Wastage		Reduction in Storage Temperature[a] Due to Assumption (°C)	
	Inert	Oxidizing	Cracking[b,c] Thickness (%)	Oxidation[c,d] Thickness (%)	Inert	Oxidizing
5	328	328	0.08	1.1	0	0
20	316	315	0.1	2.6	0	1
100	305	302	0.2	6.5	0	4
1 000	288	278	0.4	21	0	10
10 000	272	250	0.6	45	0	22

[a]Difference in temperature limit if no cladding wastage was assumed.
[b]For storage period at inert storage temperature.
[c]Based on 0.61-mm cladding thickness.
[d]For storage period at oxidizing storage temperature.

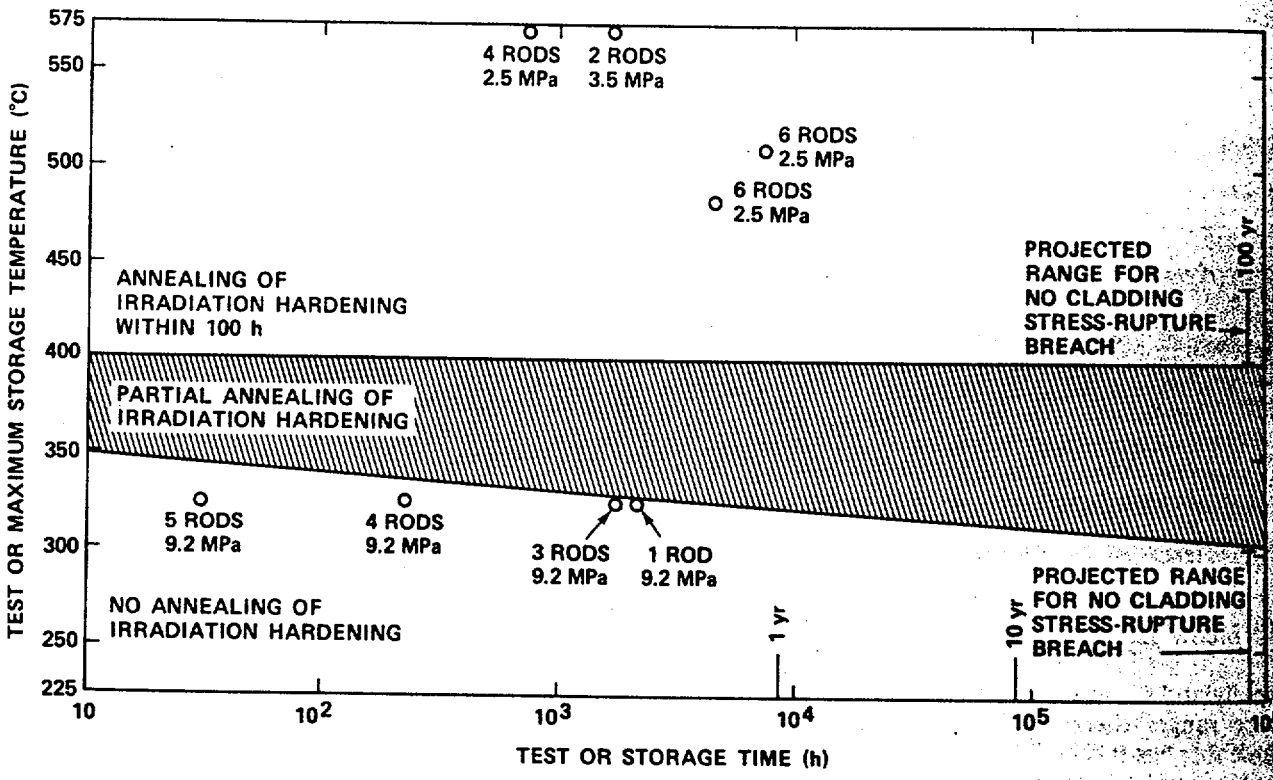

Fig. 10. Summary of accelerated whole-rod tests.

during cooldown due to loss of decay heat, the hydrogen probably precipitates as circumferential hydrides that either have little influence[25] on or even improve[31] the tensile properties of the Zircaloy at low (460 ppm H_2) hydrogen concentrations. The lifetime and temperature determinations were based on circumferential precipitation of hydrides. It is important to determine if the reorientation seen in this test will also occur under dry storage conditions, since if the hydrides reorient radially during the storage cooldown the cladding may be weakened and the form of the Larson-Miller equation[1] used in the extrapolation

may not be valid. The predicted lifetimes may be too long. Therefore, two questions must be addressed: (a) what is the critical stress for hydride reorientation, and (b) at what temperature does hydride precipitation cause premature rod breach?

The critical stress, assuming there is one, for hydride reorientation is not well defined. During specimen tests that might be typical of storage conditions (i.e., 50 to 300 ppm H_2 and soak temperatures of 300 to 400°C), reorientation generally commenced between 35 and 138 MPa (Refs. 25, 32, 33, and 34). The stress threshold was influenced by the fabrication history,[25,32] basal pole texture,[33] stressing temperature,[34] and hydrogen content.[34] There does not appear to be a dependency on the amount of time at the hold temperature due to the rapidity of the dissolution kinetics.[35,36] Cooling rate does not appear to affect the reorientation for fast cooling rates (35 to 120°C/h) (Ref. 37), but no work has been done with slower cooling rates typical of dry fuel storage. Cooling rate does affect the size of the hydrides.[28,37] As can be seen in Table VII, the hydride reorientation data on LWR rods are limited. The high-temperature and high-pressure whole-rod data indicate that the stress threshold should be between 28 and 138 MPa, which is consistent with the literature. Unfortunately, PWR rods have hoop stresses in the 200 to 300°C range of 48 to 97 MPa, the exact region of uncertainty. When a rod is taken from pool storage and put into dry storage, assuming the stress is adequate to cause the precipitating hydrides to assume a radial orientation, two things must occur before there is a hydriding problem: (a) the storage temperature must be high enough to take a sufficient amount of the circumferential hydrides into solution, and (b) the rods must cool down sufficiently to precipitate out the hydrides radially. To treat this problem in general terms is beyond the scope of this paper.

CONCLUSIONS

Turkey Point PWR Zircaloy-clad spent fuel rods were artificially pressurized to ~150 MPa and tested at 323°C for up to 2101 h to study lower temperature behavior where irradiation-hardened cladding does not anneal. The major conclusions that can be drawn from the work are:

1. If hydride reorientation does not take place, a lower bound on the maximum permissible temperature to store spent fuel isothermally in an inert atmosphere for at least 100 yr is 305°C. This temperature drops ~5°C for an oxidizing atmosphere to account for cladding oxidation. This lower bound is based on whole-rod data. Other data on spent fuel behavior in dry storage might support higher limits.

2. High-temperature tests[3] indicate that successful dry storage in an inert atmosphere for 100 yr can be accomplished if the maximum storage temperature is between 400 and 440°C,[a] since the irradiation hardening has been annealed and creep-rupture properties of unirradiated Zircaloy should be applicable. Dry storage with the maximum storage temperature between the 305°C limit for irradiation-hardened cladding and 400°C for the annealed cladding may be questioned until the creep-rupture properties of partially annealed rods have been determined.

3. Significant hydride reorientation was observed during the posttest examination. While this was probably caused by the high stress used in the test, data in the literature are not sufficiently complete to determine

TABLE VII

Pressurized Water Reactor Fuel Rod Hydride Reorientation Data

Type of Test	Room Temperature Pressure (MPa)	Stress (MPa) at 290°C	Soak Temperature (°C)	Cooldown Rate (°C/h)	Radial Hydrides (%)
Reactor shutdown[a]	3.45	~50.4	~350	30 to 50	0
High pressure whole-rod	9.25	135	323	5	50 to 90
	0	0	323	5	0
High-temperature whole-rod (Ref. 3)	1.82	26.2	482	~10	~0
	1.35	19.7	510	~10	~0
	1.06	15.5	571	~10	~0
	1.12	16.4	571	~10	~0
	1.15	16.8	571	~10	~0
	0.9	13.3	571	~10	~0

[a]Because of reactor system pressure, during cooldown the cladding would be in a compressive state.

at what stress level such hydride reorientation might occur during dry storage. Under dry storage conditions in which the fuel rod temperature is continually decreasing, precipitation of radial hydrides could provide a cladding breach mechanism that may not be present during isothermal tests. If hydride reorientation does occur during rod cooldown, then temperature limits for dry storage would have to be reevaluated.

These results were obtained on spent fuel rods that were irradiated in a typical fuel cycle in one PWR. The conclusions are thus qualified until it is determined if the test rods are typical of the general spent fuel population.

ACKNOWLEDGMENTS

The authors express their appreciation to D. A. Cantley, R. L. Knecht, L. D. Blackburn, D. Stahl, and V. Pasupathi for their many helpful discussions. The efforts of the hot-cell staff of Battelle Columbus Laboratories in performing and examining the fuel rods and Mrs. O. Merriman in typing the manuscript were also greatly appreciated.

The work was conducted at the Battelle Columbus Laboratories under the direction of Westinghouse Hanford Company for the Commercial Spent Fuel Management Program Office, which is managed by the Pacific Northwest Laboratory for the U.S. Department of Energy.

REFERENCES

1. L. D. BLACKBURN, D. G. FARWICK, S. R. FIELD, L. A. JAMES, and R. A. MOEN, "Maximum Allowable Temperature for Storage of Spent Nuclear Reactor Fuel," HEDL-TME 78-37, Hanford Engineering Development Laboratory, Richland, Washington (May 1978).

2. F. R. LARSON and J. MILLER, "A Time-Temperature Relationship for Rupture and Creep Stresses," *Trans. ASME*, **74**, 765 (1952).

3. R. E. EINZIGER, S. D. ATKIN, D. E. STELLRECHT, and V. PASUPATHI, "High Temperature Postirradiation Materials Performance of Spent Pressurized Water Reactor Fuel Rods Under Dry Storage Conditions," *Nucl. Technol.*, **57**, 65 (1982).

4. R. S. KEMPER and D. L. ZIMMERMAN, "Neutron Irradiation Effects on the Tensile Properties of Zircaloy-2," HW-52323, General Electric-Hanford Atomic Products Operation (Aug. 1957).

5. R. B. ADAMSON, "Irradiation Growth of Zircaloy," *Proc. 3rd Int. Conf. Zircaloy in the Nuclear Industry*, Quebec City, Canada, August 10-12, 1976, ASTM STP 633, p. 326, A. L. LOWE and G. W. PARRY, Eds., American Society for Testing and Materials (1977).

6. K. PETTERSSON, "Rapid Stress Corrosion Crack Growth in Irradiated Zircaloy," *J. Nucl. Mater.*, **107**, 111 (1982).

7. F. T. FUEILLO, S. PUSUHOTHAMAN, and J. C. TIEN, "Understanding the Larson-Miller Parameter," *Scripta Meta.*, **11**, 493 (1977).

8. E. HILLNER, "Corrosion and Hydriding Performance Evaluation of Three Zircaloy-2 Clad Fuel Assemblies After Continuous Exposure in PWR Cores 1 and 2 at Shippingport, PA," W-ARD-TM-1412, Westinghouse Advanced Reactors Division, Pittsburgh, Pennsylvania (Jan. 1980).

9. R. D. WATSON, "On the Oxidation of Zirconium Alloys in Air and the Dimensional Changes Associated with Oxidation," AECL-3375, Atomic Energy of Canada, Chalk River, Ontario (June 1979).

10. D. G. BOASE and T. T. VANDERGRAAF, "The Canadian Spent Fuel Storage Canister: Some Material Aspects," *Nucl. Technol.*, **32**, 60 (Jan. 1977).

11. D. A. WOODFORD, "Creep Analysis of Zircaloy-4 and Its Application in the Prediction of Residual Stress Relaxation," *J. Nucl. Mater.*, **79**, 345 (1979).

12. H. E. ROSINGER and P. C. BERA, "Steady-State Creep of Zircaloy-4 Fuel Cladding from 940 to 1873 K," *J. Nucl. Mater.*, **82**, 286 (1979).

13. D. L. HAGRMAN and G. A. REYMANN, "MATPRO-Version 11, A Handbook of Materials Properties for Use in the Analyses of Light Water Reactor Fuel Rod Behavior," NUREG/CR-0497, U.S. Nuclear Regulatory Commission, Washington, D.C. (Feb. 1979).

14. K. R. MERCKX, "Calculational Procedures for Determining Creep Collapse of LWR Fuel Rods," *Nucl. Eng. Des.*, **31**, 95 (1974).

15. P. J. PANKASKIE, "Irradiation Effects on the Mechanical Properties of Zirconium and Dilute Zirconium Alloys: A Review," BN-SA-618, p. 47, Battelle Pacific Northwest Laboratories, Richland, Washington (July 1976).

16. D. E. STELLRECHT, V. PASUPATHI, and J. C. KROGNESS, "Elevated Temperature Testing of Spent Nuclear Fuel Rods," Trans. Am. Nucl. Soc., **34**, 839 (June 1980).

17. R. B. DAVIS, "Data Report for the Nondestructive Examination of Turkey Point Spent Fuel Assemblies B01, B03, B17, B41 and B43," HEDL-TME 79-68, Hanford Engineering Development Laboratory, Richland, Washington (May 1980).

18. S. D. ATKIN, "Destructive Examination of 3-Cycle LWR Fuel Rods from Turkey Point Unit 3 for the Climax Spent Fuel Test," HEDL-TME 80-89, Hanford Engineering Development Laboratory, Richland, Washington (June 1981).

19. R. B. DAVIS, "Pre-Test Nondestructive Examination Data Summary Report on Turkey Point Spent Fuel Assemblies D01, D04, D06 for the Climax Spent Fuel Test," HEDL-TME 80-83, Hanford Engineering Development Laboratory, Richland, Washington (June 1981).

20. R. B. DAVIS and V. PASUPATHI, "Data Summary Report for the Destructive Examination of Rods G7, G9, J8, I9 and H6 from Turkey Point Fuel Assembly B17," HEDL-TME 80-85, Hanford Engineering Development Laboratory, Richland, Washington (Apr. 1981).

21. F. L. YAGGEE, R. F. MATTAS, and L. A. NEIMARK, "Characterization of Irradiated Zircaloys: Susceptibility to Stress-Corrosion Cracking," EPRI NP-1155, Electric Power Research Institute, Palo Alto, California (Sep. 1979).

22. D. CUBICIOTTI and R. L. JONES, "EPRI-NASA Cooperative Project on Stress-Corrosion Cracking in Zircaloys," EPRI NP-717 Electric Power Research Institute, Palo Alto, California (Mar. 1978).

23. A. B. JOHNSON, E. R. GILBERT, and R. J. GUENTHER, "Behavior of Spent Nuclear Fuel and Storage System Components in Dry Interim Storage," PNL-4189, Pacific Northwest Laboratory, Richland, Washington (Aug. 1982).

24. A. TASOOJI, R. E. EINZIGER, and A. K. MILLER, "Modelling of Zircaloy Stress Corrosion Cracking: Texture Effects and Dry Storage Spent Fuel Behavior," *Proc. 6th ASTM Symp. Zirconium in the Nuclear Industry*, Vancouver, British Columbia, June 1982, ASTM STP-824, D. G. FRANKLIN and R. B. ADAMSON, Eds., American Society for Testing and Materials (Aug. 1984).

25. M. R. LOUTHAN, Jr. and R. P. MARSHALL, "Control of Hydride Orientation in Zircaloy," *J. Nucl. Mater.*, **9**, *2*, 170 (1963).

26. M. R. LOUTHAN, Jr. and C. L. ANGERMAN, "The Influence of Stress on the Hydride Habit Plane in Zircaloy-2," *Trans. TMS-AME*, **236**, 221 (1966).

27. "MATPRO Version 10, A Handbook of Materials Properties for Use in the Analyses of LWR Fuel Rod Behavior," TREE NUREG-1180, EG&G Idaho, Inc., Idaho Falls, Idaho (Feb. 1978).

28. C. E. ELLIS, "Hydride Precipitates in Zirconium Alloys," *J. Nucl. Mater.*, **28**, 129 (1968).

29. R. P. MARSHALL and M. R. LOUTHAN, Jr., "Tensile Properties of Zircaloy with Orientated Hydrides," *Trans. ASM*, **56**, 693 (1963).

30. E. D. HINDLE, "Effect of Circumferentially Aligned Hydrides on the Ductility of Zircaloy-2 Tubing Under Biaxial Stress," *J. Inst. Metals*, **95**, 359 (1967).

31. K. VIDEM, "Properties of Zirconium Base Cladding Materials—Corrosion and Hydrogen Pickup," *Nucl. Eng. Des.*, **21**, 200 (1972).

32. R. P. MARSHALL, "Influence of Fabrication History on Stress-Oriented Hydrides in Zircaloy Tubing," *J. Nucl. Mater.*, **24**, 34 (1967).

33. D. O. PICKMAN, "Properties of Zircaloy Cladding," *Nucl. Eng. Des.*, **21**, 212 (1972).

34. D. HARDIE and M. W. SHANAHAN, "Stress Reorientation of Hydrides in Zr-2.5%Nb," *J. Nucl. Mater.*, **55** (1975).

35. G. P. WALTERS, "Hydride Morphology in Stressed Zirconium," AERE R-5045, Atomic Energy Research Establishment, Harwell, U.K. (Sep. 1965).

36. G. W. PARRY, "Stress Reorientation of Hydride in Cold-Worked Zr-2.5%Nb Pressure Tubes," AECL-2624, Atomic Energy of Canada, Chalk River, Ontario (Aug. 1966).

37. D. O. NORTHWOOD and U. KOSASIH, "Hydrides and Delayed Hydrogen Cracking in Zirconium and Its Alloy," *Int. Metall. Rev.*, **28**, *2*, 92 (1983).

MODELLING OF THE MECHANICAL BEHAVIOUR OF ZIRCALOY-4 CLADDING TUBES FROM UNIRRADIATED STATE TO HIGH BURN-UP

I. Schäffler-Le Pichon
EDF /DER /MTC
Route de Sens
BP1, 77250 Moret Sur Loing, France
01 60 73 70 81

Ph. Geyer
EDF /DER /MTC
Route de Sens
BP1, 77250 Moret Sur Loing, France
01 60 73 72 69

P. Delobelle
Laboratoire de Mécanique Appliquée R. Chaléat,
U.A. CNRS,
25030 Besançon, France
03 81 40 29 13

P. Bouffioux
EDF /DER /EMA
Route de Sens
BP1, 77250 Moret Sur Loing, France
01 60 73 63 05

ABSTRACT

We proposed in this paper a viscoplastic model able to simulate nonisothermal out-of-flux mechanical behavior of Zircaloy-4 CWSR cladding tubes irradiated until high burn-up. This model without threshold imposed to use three kinematical hardening variables to simulate the strong nonlinearity of the mechanical behavior. Some modifications of the model are justified by the evolution of the mechanical behavior of cladding tubes due to irradiation. Finally, results of numerical simulations show the ability of the model to reproduce biaxial tensile, high hoop stress levels creep and recovery tests performed at 350, 380 and 400°C on cladding tubes irradiated to different fast neutron fluences levels between 0 and 85.10^{24} n/m^2.

I. INTRODUCTION

As more than 75 % of electricity in France is generated by nuclear energy, the French PWR have an important role in the grid regulation. Load follow has become a normal operating mode. In addition, EDF wants to increase the discharge burn-up of the fuel sub-assemblies to about 60 GWd/tU. Those operating conditions lead to numerous pellet cladding interaction (PCI) transients. In order to improve the accuracy of the stress-strain level in the cladding, a new model to describe the anisotropic viscoplastic behavior of the irradiated Zircaloy-4 cladding tubes has been developed. To reach this aim a mechanical data basis of experimental tests carried out out-of-flux on irradiated materials is required. EDF contributes with lots of industrial partners to its constitution.

First, we present the constitutive equations of the model. The ability of the model to simulate the viscoplastic behavior of non-irradiated CWSR

Zircaloy-4 cladding tubes between 350 and 400°C under uniaxial and biaxial loadings is illustrated. The application of the model to simulate complex loadings representative of a PCI transient is also presented.

Then, the analysis of biaxial tension and creep tests carried out on cladding tubes irradiated to five different fluences levels between 4.10^{24} n/m^2 and 85.10^{24} n/m^2 (E > 1 MeV) shows an irradiation hardening of the cladding tubes and a decrease in creep deformation.
Irradiation effects are then introduced into this model through an internal state variable of damage, which is a function of the fluence. This variable imposes an increase of the kinematical hardening and a decrease of the static recovery but does not modify the description of anisotropy. This new formulation is identified on monotonous tensile and creep tests performed at 350°C on irradiated cladding tubes, and validated at 380 and 400°C.

II. TESTED MATERIALS AND EXPERIMENTAL RESULTS

A. Tested Materials

Mechanical tests have been carried out on CWSR cladding tubes with nominal dimensions 9,5 mm outside diameter and 0,57 mm wall thickness. The chemical composition of these tubes measured is given in table1. The content of alloying elements is consistent with the ASTM B353 specification.

Table 1. Weight composition of Zircaloy-4

Alloying elements (%)					Impurities (ppm)		
Cr	Fe	Sn	O	Zr	C	N	H
0,10	0,21	1,25	0,11	bal.	120	31	<2

The texture analysis reveals a fairly pronounced anisotropy. The Kearns factors show the radial trend for the crystallographic texture (f_r = 0,57; f_a = 0,35; f_t = 0,08, in radial, tangential and longitudinal directions respectively). By assuming that the structure axes are identical with the anisotropic axis, then the tube has an orthotropic mechanical behavior.

B. Mechanical Tests Realized on Unirradiated CWSR Cladding Tubes

Monotone axial tension tests have been performed at 350 and 400°C for different strain rates between 2.10^{-6} and 2.10^{-3} s^{-1}. The experimental tests reveal the strong viscosity of the material at those temperatures. The Rp ratio is used to illustrate the anisotropy of the tubes. Rp is the ratio of the plastic hoop strain and the axial one. Rp is found to be independent of temperature and strain rates. To simplify the description of anisotropy in the model, the set of anisotropy coefficients will be considered in a first approximation as independent of temperature and strain rate, which corroborates the results of Beauregard and al. [1] and Murty[2].

To characterized the anisotropy of these tubes biaxial tensile tests are realized for different stress-biaxiality ratio (hoop stress divided by longitudinal stress). These tests are carried out with a machine which allows us to imposed a stress-biaxiality ratio. The imposed hoop strain rate is measured by diametral extensometers. The machine adapts the oil pressure and also the hoop stress to maintain the fixed hoop strain rates. Knowing the hoop stress, it imposes the longitudinal stress to ensure the value of the biaxiality ratio. Uniaxial (140 MPa < σ_z < 400 MPa) and biaxial creep tests (100 MPa < σ_θ < 275 MPa are realized, too.

C. Mechanical Tests Realized Out-of-flux on Irradiated CWSR Cladding Tubes

Biaxial tests (α = 0.5) are realized on irradiated CWSR cladding tubes irradiated until fluences range 0-85.10^{24} n/m^2 (E > 1 MeV). Biaxial tensile tests are realized at 350, 380°C and 400°C for different strain rates between $1,4.10^{-7}$ s^{-1} and 2.10^{-4} s^{-1}. These tests are completed by creep tests realized at 350, 380°C and 400°C for imposed hoop stress between 270 and 550 MPa.

III. MODELING OF UNIRRADIATED ZIRCALOY-4

A. A Unified Viscoplastic Model

By admitting the case of small strain, the strain can be split up into two terms: an elastic deformation ε^e considered isotropic and a viscoplastic deformation ε^{vp}. The Young Modulus E(T) is linearly temperature dependent between 350 and 400°C.

$$[\varepsilon] = [\varepsilon^e] + [\varepsilon^{vp}] \quad (1)$$

$$[\varepsilon^e] = \frac{1+\upsilon}{E(T)}[\sigma] - \frac{\upsilon}{E(T)}\mathrm{Tr}(\sigma)[I] \quad (2)$$

We consider the existence of a viscous stress σ_v. The stress σ is the sum of two components, a viscous stress and an internal stress α.

Classically, an orthotropic anisotropy such as Hill's one can be proposed [6]. Experimental studies including cyclic tests clearly indicated the kinematical nature of the hardening [7]. Then we propose this equation

$$\overline{\sigma - \alpha} = \left(\frac{3}{2}(\sigma' - \alpha')^t [\underline{M}] (\sigma' - \alpha')\right)^{1/2} \quad (3)$$

to describe the equipotential surfaces of the thermodynamical potential. $\overline{\sigma}$ is the equivalent stress, $[\underline{M}]$ a matrix of anisotropy, α' the deviatoric kinematical hardening variable and σ' the deviatoric stress tensor.

Ahlquist and Nix[3] used a stress dip test technique to estimate the variations of σ_v with the equivalent cumulated plastic strain rates $\dot{v}$. This technique applied on Zircaloy tubes, although experimentally imprecise, allows Delobelle and Robinet[4] to determine the form of the biunivoc relation between these two terms (4). This equation is the same that the one proposed by Miller for Zircaloy 2 cladding tubes[5].

$$\dot{v} = \dot{\varepsilon}_0(T)\left\{\sinh\left(\frac{\sigma_v}{N(T)}\right)\right\}^n \text{ with} \quad (4)$$

$$\begin{cases} N(T) = cT + d \\ \dot{\varepsilon}_0(T) = m\exp(-\Delta H / kT)\left(N(T)^n\right) \end{cases}$$

ΔH is the activation energy, T the temperature and k the Boltzmann's constant. The Maxwell Boltzmann statistic describes the evolution of some parameters with the temperature according to an Arrhenius law.

The application of the normality rule gives us the viscoplastic deformation (5). The model equations are written according to:

$$\left[\dot{\varepsilon}^{vp}\right] = \frac{3}{2}\,\dot{v}\,\frac{[\underline{M}]\left[\sigma' - \alpha'\right]}{\bar{\sigma} - \bar{\alpha}} \qquad (5)$$

Because the tubes can be considered as an orthotropic medium, the anisotropic behavior of theses ones is described by a matrix composed of nine components. The loadings do not imposed shear, then the matrix is reduced to six components.
The choice of the longitudinal direction as a reference direction, the uniaxial and biaxial tensile tests, and the three incompressibility relations (by neglecting the value of α in (4)) determine the matrix $[\underline{M}]$ [9].

The evolution laws of the kinematical hardening variables α, $\alpha^{(1)}$ and $\alpha^{(2)}$ (6,7,8) define the mechanical behavior completely. Three kinematical variables are necessary to simulate the strong nonlinearity of the mechanical behavior of Zircaloy. The first term of these equations is the linear part of the hardening, the second term represents the dynamic recovery, and the last one represents the time dependent static recovery. The anisotropic mechanical behavior of these different phenomenons is taken into account respectively by three others tensors, $[\underline{N}]$, $[\underline{Q}]$ and $[\underline{R}]$.

Y is a scalar variable associated with the increase of the total dislocation density in the material.

$$\left[\dot{\alpha}'\right] = p\left(\frac{2}{3}\,Y(v)[\underline{N}]\left[\dot{\varepsilon}^{vp}\right] - [\underline{Q}]\left[\alpha' - \alpha'^{(1)}\right]\dot{v}\right) - r_m(T)\sinh\left(\left(\frac{\bar{\alpha}}{\alpha_0(T)}\right)^{m_0}\right)[\underline{N}][\underline{R}]\frac{\left[\alpha'\right]}{\bar{\alpha}} \qquad (6)$$

with

$$\begin{cases} r_m(T) = p\exp\left(-\Delta H^* / kT\right)\alpha_0(T) \\ \alpha_0(T) = qT + s \end{cases}$$

$$\left[\dot{\alpha}'^{(1)}\right] = p_1\left(\frac{2}{3}\,Y(v)[\underline{N}]\left[\dot{\varepsilon}^{vp}\right] - [\underline{Q}]\left[\alpha'^{(1)} - \alpha'^{(2)}\right]\dot{v}\right) \qquad (7)$$

$$\left[\dot{\alpha}'^{(2)}\right] = p_2\left(\frac{2}{3}\,Y(v)\,[\underline{N}]\left[\dot{\varepsilon}^{vp}\right] - [\underline{Q}]\left[\alpha'^{(2)}\right]\dot{v}\right) \qquad (8)$$

$$\text{with } \bar{\alpha} = \sqrt{\frac{3}{2}\,\alpha'\,\underline{R}\,\alpha}$$

$$\dot{Y} = b\left(Y^{sat} - Y\right)\dot{v}\,;\; Y(0,T) = aT + c$$

B. Identification of the Model and Simulations

The parameters of the model are obtained by numerical simulations on uniaxial and biaxial tensile and creep tests at 350 and 400°C. The adequation between the simulations and the experimental tests shows the ability of the model to simulate uniaxial and biaxial tensile, creep, and relaxation tests for temperatures between 350 and 400°C. The evolution of parameter with the temperature are verified by comparing simulations with tests results at 380°C [8,9]. On fig.1, the model is in good agreement with tensile tests ($\alpha = \sigma_\theta/\sigma_z = 0.5$) with an imposed hoop strain rate of $2.10^{-5}s^{-1}$ followed by a relaxation test. The same adequation between tests and prediction has been obtained for an imposed strain rate of 2.10^{-4} s^{-1}. These two hoop strain rates frame the one imposed by the pellet on the cladding tubes during an interaction.

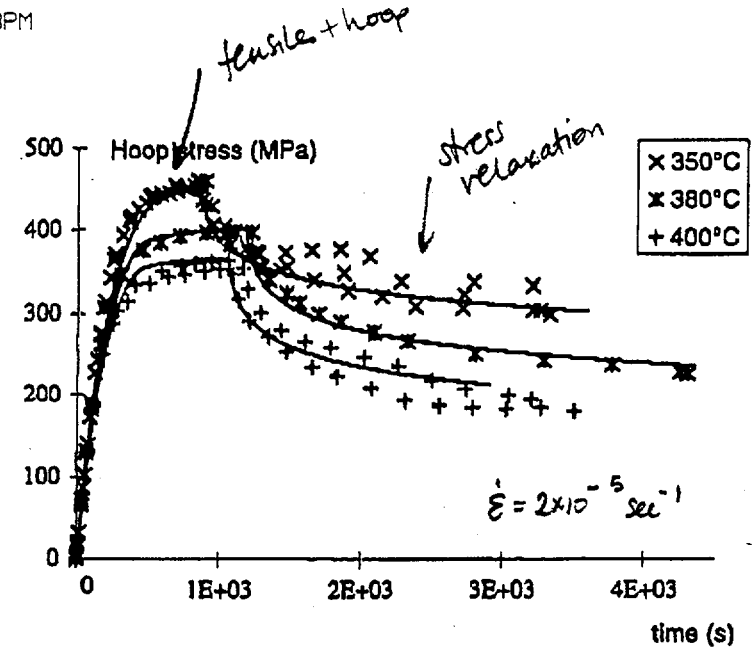

Fig.1 Complex loadings and simulations at different temperatures

IV. MODELING OF IRRADIATED ZIRCALOY-4

A. Post-Irradiation Testing

During the mechanical tests, the temperature and the stress level are known with an accuracy of about 5°C and 10 MPa (respectively).

The elastic behavior of the cladding tubes does not change with the irradiation. If σ_{ec} is the flow stress of the material for an among of total deformation, the variation for the entire range of fluences shows the irradiation hardening of the material (Figure 2). The irradiation hardening is significant until 45.10^{24} n/m^2. After this fluence level, the evolution tensile behavior is not so pronounced.

During the secondary creep, we considered that the hardening of the material is constant and the viscous stress small. Then the evolution law of the kinematical hardening variable (eq.6) can be write:

$$\dot{v} = r^*(T)\sinh\left(\frac{\bar{\alpha}}{\alpha^*_0(T)}\right)^{m_0} \qquad (9)$$

This remark is illustrated by the figure 3. The secondary creep strain rate divided by a constant is drown versus of the creep stress. This strain rate is linked to the static recovery ability of the material (see, eq.9). When the fluences increase, the strain rate decreases for the same stress level. The static recovery decreases quickly with the irradiation until a fluence of about 45.10^{24} n/m^2 and after this the evolution is slower.

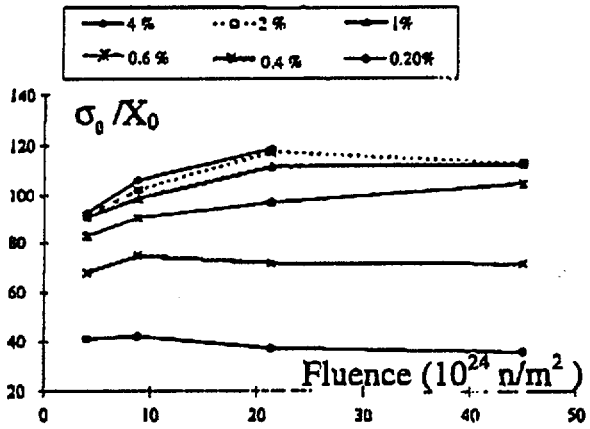

Fig. 2 - Variation of the flow stress divided by a constant as a function of fluence during a biaxial tensile test realized for an imposed hoop strain rate of 5.10^{-5} s^{-1} at 350°C.

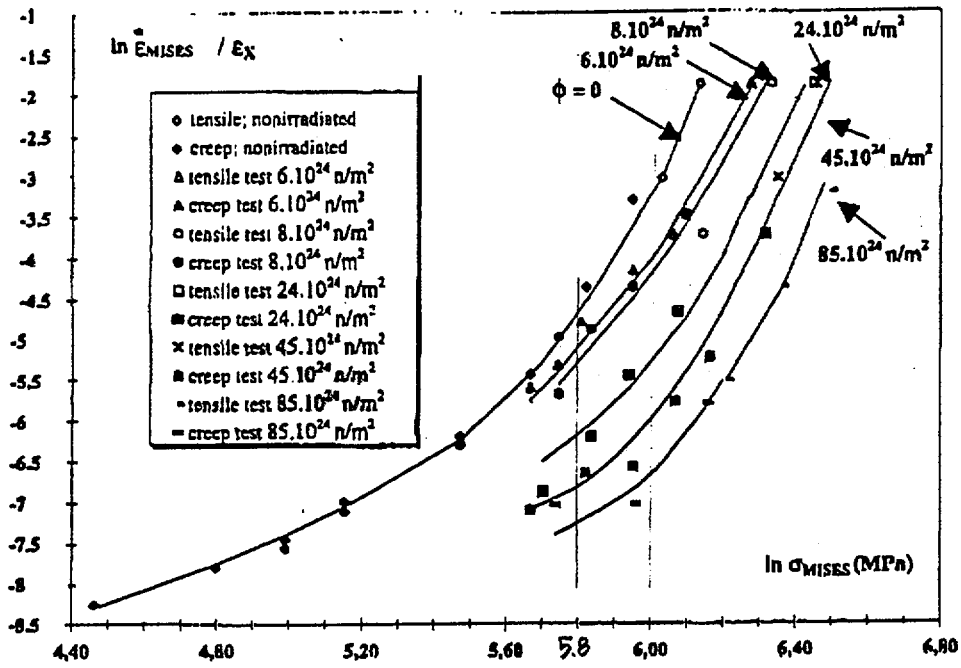

Fig. 3 - Equivalent secondary creep strain rates versus equivalent stress at 350°C

To illustrate the thermal creep strength of the material we can draw on the figure 4 the secondary strain rate versus of the fluences for different stress levels.

The study of the experimental results shows an irradiation hardening of the cladding tubes and a decrease in creep deformation. These changes in mechanical properties due to irradiation are significant until 45.10^{24} n/m². After this fluence level, the evolution of mechanical behavior is not so pronounced. All our results confirmed the ones of Baty et al.[10] .

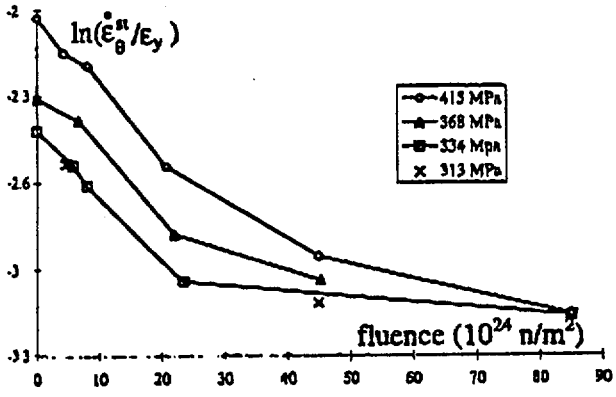

Fig.4- Equivalent secondary creep strain rates versus fluence at 350°C

To take into account the irradiation damage, we introduce the scalar variable D defined by:

$$D(\phi) = a\,(1 - \exp(-h\phi)) \qquad (10)$$

where ϕ is the fluence.

We propose to modify the terms $r_m(T)$ and $\alpha_0(T)$ with the irradiation in order to allow the translation of the curve (fig.3).

$$\begin{cases} r_m(T,D) = r_m(T)\exp(-\chi D^\gamma) \\ \alpha_0(T,D) = \alpha_0(T)\exp(-\eta D^\beta) \end{cases} \qquad (11)$$

We make the same for the state equation (eq.4).

$$\begin{cases} \dot{\varepsilon}_0(T,D) = \dot{\varepsilon}_0(T)\,N(T,D)^n \exp(-\xi D^\varepsilon) \\ N(T,D) = N(T) + \mu(1 - \exp(-\Gamma D)) \end{cases} \qquad (12)$$

B. Identification and Simulation of the Out-of-flux Behavior of CWSR Cladding Tubes

This new formulation is identified on monotonous biaxial tensile and creep tests (335 MPa < $\sigma_\theta - \sigma_r$ < 550 MPa) performed at 350°C on irradiated cladding tubes, and validated at 380 and 400°C. The

figure 5 illustrates the capability of the model to simulate biaxial tensile tests at 350°C for different fluences. On the figure 6 we compare the calculation with a recovery tests realized at 350°C.

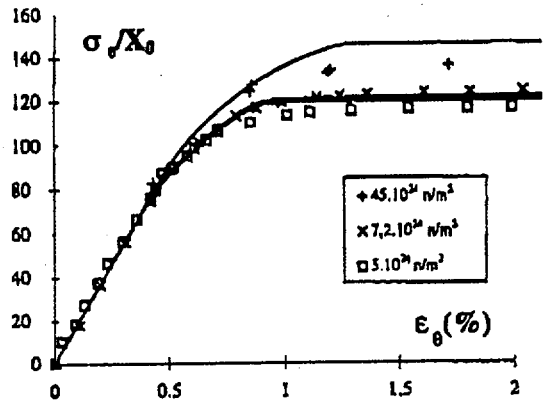

Fig.5 - Biaxial tensile tests realized at 350 °C for an imposed hoop strain rate of 2.10^{-4} s^{-1} for different fluences and simulations.

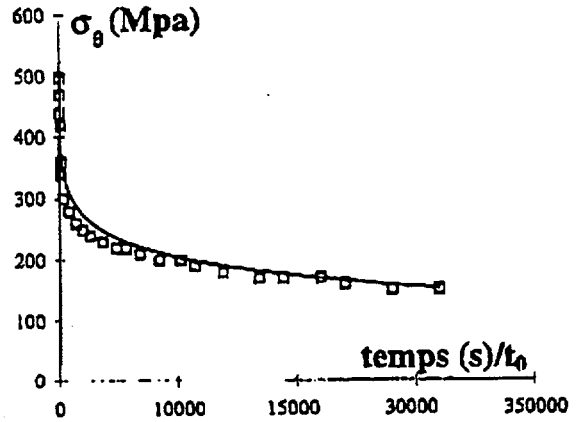

Fig.6- Recovery test; Fluence 7.10^{24} n/m^2; Hoop strain rate $\dot{\varepsilon}_\theta = 4.10^{-4}$ s^{-1}

The figures 7 and 8 show that the model is able to predict the mechanical behavior of irradiated cladding tubes at 380 and 400°C.

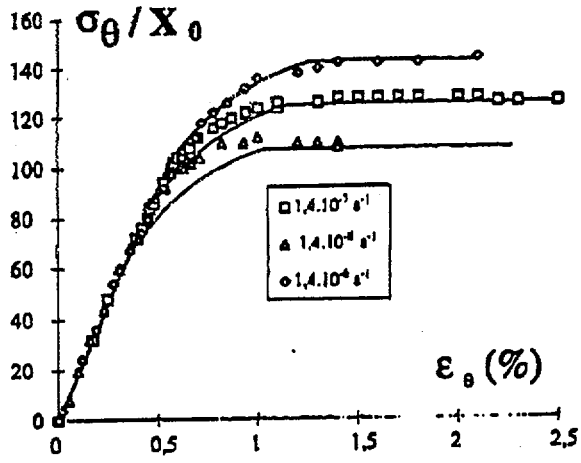

Fig.7- Biaxial tensile tests realized at 380°C on cladding tubes irradiated until 85.10^{24} n/m^2.

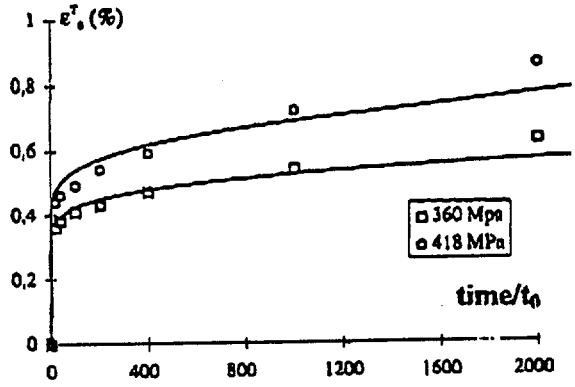

Fig.8- Biaxial creep tests realized at 380°C on cladding tubes irradiated until 45.10^{24} n/m^2.

V. CONCLUSIONS

The analysis of the out-of-flux experimental data basis composed of biaxial tensile, creep and recovery tests carried out on irradiated CWSR cladding tubes shows the hardening and a decrease in creep deformation due to irradiation. These irradiation effects are introduced into this model through an internal state variable of damage, which is a function of the fluence. This variable imposes an increase of the kinematical hardening and a decrease of the static recovery but does not modify the description of anisotropy. Finally, we show the ability of the modeling to calculate the anisotropic behavior of cladding tubes during tensile, high hoop stress levels creep and relaxation tests in the temperature range 350-400°C, and fluences range 0-85.10^{24} n/m^2 (E > 1 MeV). This model is already introduced in the EDF finite element Code_Aster® and will be implemented in the cladding tube calculation code of EDF Cyrano3

(Delobelle-Schaeffler model) to allow the calculation of PCI transcients.
Future developements of this model will concern "irradiation creep". Then, a research programm supervised by CEA, Framatome and EDF (in-pile creep at high stress levels of Zircaloy-4 cladding tubes) will permit to evaluate the eventuel effects of instantaneous fast neutron flux.

ACKNOWLEDGMENTS

The authors want to thank their industrial partners for financial and technical supports in the R&D programs used to develop this model. In particularly, we wants to thank Framatome Nuclear Fuel for supplying the material on which that study has been conducted, Commissariat à l'Energie Atomique for having carried out the experimental tests on irradiated materials as well EDF/SEPTEN for its financial support of this work.

REFERENCES

1. R.J. Beauregard, J.S. Clevinger and K.L. Murty, "Effect of Annealing Temperature on the Mechanical Properties of Zircaloy-4 Cladding" *Proc. SMIRT IV*, paper C3/5, (1977).
2. K.L. Murty, "Applications of Cristallographic Textures of Zirconium Alloys in Nuclear Industry" *Proc. Zirconium in the Nuclear Industry VIII Symposium*, ASTM STP, 1023, 570 (1989).
3. C.N. Ahlquist and W.D. Nix, "A Technique for Measuring Internal Stress during High Temperature Creep", *Scripta Metall.*, 3, 679 (1963).
4. P. Delobelle and P. Robinet, "Etude du Comportement et de la modélisation viscoplastique du Zircaloy-4 recristallisé sous chargements monotones et cycliques uni- et biaxés", *Journal de Physique III*, 4, 1347 (1994).
5. Miller, A.K., *Unified constitutive equations for creep and plasticity*, pp.140-151, Elsevier applied science, ed., London & New York (1987).
6. R. Hill, *The Mecanical Theory of Plasticity*, Clarendon Press, Oxford (1950).
7. P. Robinet, *Etude expérimentale et modélisation du comportement viscoplastique anisotrope du Zircaloy-4 dans deux états métallurgiques*, Thesis presented at the University of Franche-Comté (1995).
8. I. Le Pichon, Ph. Geyer, P. Bouffioux and P. Delobelle, "A Unified Constitutive Model to describe the Anisotropic Viscoplastic Behavior of Zircaloy-4 Cladding Tubes", *Proc. of the third Asia Pacific Symposium*, pp. 247-253, AEPA'96 (1996).
9. P. Delobelle, P. Robinet, Ph. Geyer, P. Bouffioux and I. Le Pichon, "A unified model to describe the anisotropic viscoplastic behaviour of Zircaloy-4 cladding tubes", *11th Symposium of the ASTM STP*, Garmich Partenkirchen, Germany, ASTM STP, 1295, (1995).
10. D.L. Baty, W.A. Pavinitch, M.R. Dietrich, G.S. Clevinger and T.P. Papazoglou, "Deformation Characteristics of Cold-worked and Recristallized Zircaloy-4 Cladding", *6th Int. Symp. ASTM STP*, pp. 306-339, ASTM STP, 824, (1984).